Variation of the Peak Gust Speed Over an Isolated Hill

A thesis presented for the Degree of

Master of Engineering in the

University of Canterbury

By

Hong Clucas, B.E.

Department of Mechanical Engineering,
University of Canterbury,
Christchurch,
New Zealand.

February 1991

ABSTRACT

This thesis describes the behaviour of the peak-gust speed over an isolated hill by studying wind tunnel models.

A brief description of relevant background theory from literature has been summarised.

The Askervein Hill model which had been used previously in several tests for the Askervein Hill Project was reused in this project. Measurements of the mean wind speeds, RMS velocity and the gust factors at different averaging time were made over the Askervein Hill model at 10 metres height and 1, 2 and 3 hill heights.

Experimental evidence shows that the gust factors in the attached flow over a simple isolated hill are directly related to the local turbulence intensity and are largely independent of special hill effects. The values indicated by the New Zealand and Australian Draft Building Codes for the variation in mean wind and gust speed topographic multipliers over a low isolated hill were compared with the experimental data. It shows that both Codes appear adequate for the example considered.

Acknowledgements

I wish to acknowledge my appreciation for the generous help and encouragement contributed to me by many people throughout this project.

I wish to express my thanks to Dr. A. J. Bowen for his conscientious and enthusiastic supervision of this project and for his continual encouragement, friendship and interest which will always be fondly remembered.

My sincere thanks to the technical staff of the Department of Mechanical Engineering who have provided valuable assistance, in particular Mr. G. Harris and Mr. P. Smith.

The financial support of the Building Research Association of New Zealand is also gratefully acknowledged.

I would like to thank my parents and Mr. J. Gray for their help and support.

Finally, the project could not have been successfully completed without the help and encouragement of my dear husband Donald.

LIST OF CONTENTS

LIST OF FIGURES

LIST OF TABLES

LIST OF SYMBOLS

A	arbitrary constant. function of turbulence intensity used in gust speed analysis.
A_z	amplification factor = $U(\Delta z)/U_0(\Delta z)$.
a	scale factor in distribution of extreme values. arbitrary constant.
B	arbitrary constant.
C_g	geostrophic drag coefficient = $(U_*/U_{10})^2$.
CDF	cumulative distribution function.
c	arbitrary constant.
D	dimension.
D_{str}	size of the structure or structural element.
d_{gust}	'size' of a typical gust used by Taylor's Hypothesis.
e	natural logarithmic base, 2.7183.
f	frequency, radians/second.
G	gust factor.
ΔG	mean gust speed fractional speed-up.
g	peak factor.

$g(x)$ monotonic increasing function of x used in distribution functions.

H hill height.

K_{10} surface drag coefficient at a height of 10m, i.e. $K_{10} = (U_*/U_{10})^2$.

K_t topographic type factor

k Von Karman constant = 0.4
Weibull probability distribution constant.

L distance from the hill crest to where the hill height is half its maximum value.

L_d horizontal length of downwind hill slope.

L_e characteristic hill length or distance from the ridge to a level half the height below the crest in the direction of the wind.

L_m hill model size.

L_f full scale hill size.

L_u horizontal length of upwind hill slope.

^xL_u the longitudinal integral length scale of the turbulence.

l thickness of inner layer.

$\overline{M}_t$ mean wind speed topographic multiplier.

$\hat{M}_t$ mean gust speed topographic multiplier.

m rank of the extreme value used in the extreme value

analysis.

N	number of samples in each data set.
n	arbitrary constant. frequency, Hz.
P(x)	probability of the variate less than x.
P(V)	probability of a speed less than V.
$P_X(x)$	CDF of a parent distribution as being of a variate,X taking on values, x.
$P_Y(y)$	Type 1 extreme value distribution.
PDF	probability density function.
$S_u(n)$	longitudinal velocity power spectral density function.
ΔS	fractional mean-wind speed-up.
T	sampling time used in equation 4.2.
T_{av}	averaging time.
T_0	length of time over which data is averaged or length of data file.
t	time. gust averaging time used in equation 4.2, 4.3.
U	mode of the distribution.
$U_0(\Delta z)$	undisturbed or upstream wind profile.

$U(t)$ instantaneous wind velocity in longitudinal direction along the mean wind direction.

U_* surface friction velocity.

Ur reference mean velocity.

ΔU velocity perturbation = $U(x,y,\Delta z) - U_0(\Delta z)$

$u, u(t)$ instantaneous longitudinal wind velocity component.

V instantaneous velocity in streamwise direction.

$\overline{V}$ mean velocity speed at height, Z.

$\hat{V}$ peak gust velocity.

$v, v(t)$ instantaneous lateral wind velocity component.

$w, w(t)$ instantaneous vertical wind velocity component.

X variate of the parent distribution (taking on values x) used in Type 1 distribution.

x distance downstream of the bar grid.

Y largest value of X

y reduced variate used in extreme values analysis.

Z_0 surface roughness length.

Z boundary-layer thickness.

z height above datum level on flat surrounding terrain.

Δz height above the local terrain.

α power-law exponent.

$\hat{\eta}$ mean factor = $(\hat{V} - \bar{V})/\sigma_v$.

ν measure of the average frequency of extreme gusts.

ρ air density.

$\sigma_u, \sigma_v, \sigma_w$ standard deviation of fluctuating wind velocity components u, v and w.

Φ effective upwind slope of the hill.

Φ_d effective down-wind slope, measured from the crest of a hill to the datum level in the direction of the wind.

CHAPTER 1

INTRODUCTION

The variation of the mean-wind speed over smooth isolated hills is now fairly well understood and can be predicted with reasonable accuracy. However for rigid structures not susceptible to dynamic effects, the New Zealand Building Code (NZS 4203) along with many others still use the quasi-static approach to predict the maximum gust loading which requires knowledge of the peak-gust speed.

1.1 AIM OF THE PROJECT

The aim of this project is to understand the behaviour of the peak-gust speeds over an isolated hill by examining model data files of air flow over an isolated model hill in the low speed wind-tunnel of the University of Canterbury. In particular a comparison has been made with the peak-gust values defined in the new Draft Building Codes of New Zealand (2/DZ 4203,1989) & (2/DZ 4203/1,1991) and Australia (DR 87163,1987).

1.2 PROJECT BACKGROUND

It was well known that New Zealand is endowed with high winds in many parts of the country, (Fig 1.1 shows the local wind patterns.) therefore the problems of wind effects over complex terrain is of particular concern to New Zealand. Correct estimations of the wind speeds over complex terrain for design purposes is seen therefore to be of great importance to local engineers.

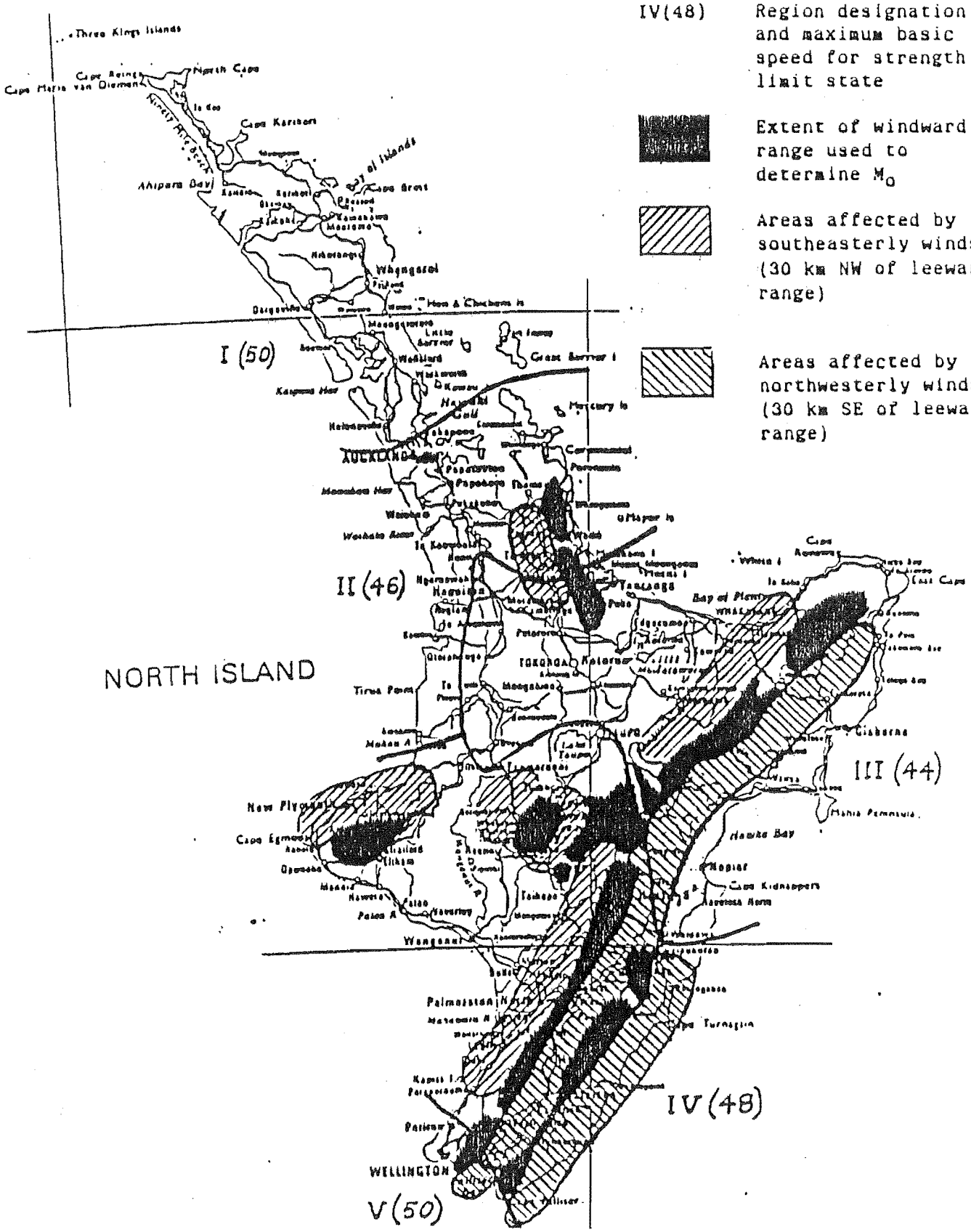

Fig. 1.1a North Island Local Wind Patterns.
2/DZ 4203 (1991)

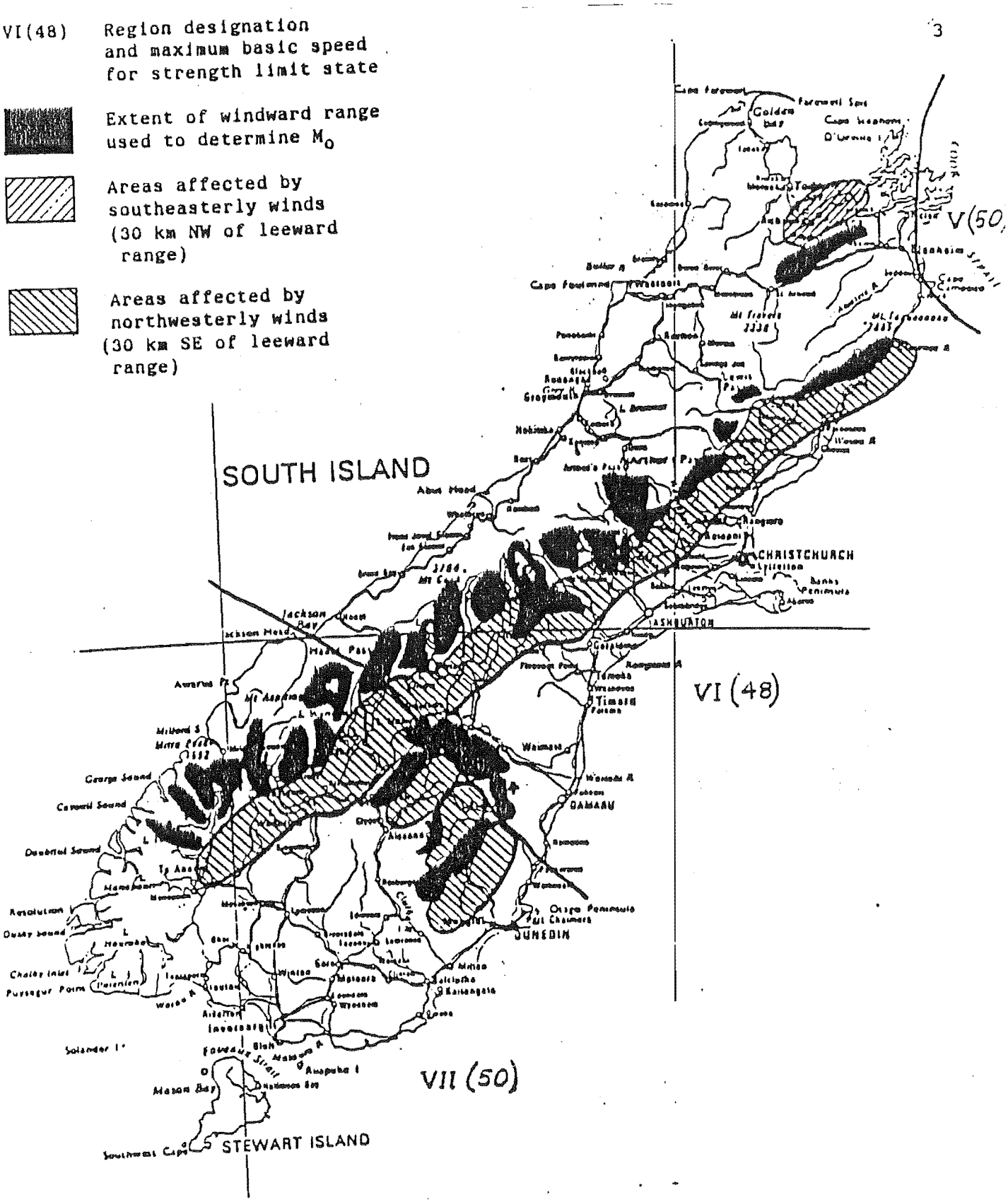

Fig 1.1b South Island Local Wind Patterns.
2/DZ 4203 (1991)

Over the last few years, the study of mean-wind speed over an isolated hill < Askervein Hill > was carried out by the International Energy Agency Program of Research and Development on Wind Energy Conversions Systems (WECS). They concentrated on the measuring the spatial characteristics of mean wind and turbulence over a typical WECS hill site and further understanding of boundary-layer flow over relatively low hills. A significant amount of data for mean-wind speeds is available, but there are no data on the behaviour of the peak-gust speeds. As the basic part of the assessment of wind loads on structures is the prediction of the extreme wind and the risk of it being exceeded, it was thought that more investigations should be focused on the peak-gust speeds by wind-tunnel model studies.

With the financial help of the Building Research Association of New Zealand, the research of peak-gust speeds over an isolated hill was undertaken in the Department of Mechanical Engineering, University of Canterbury and the results along with their interpretations are published in this thesis.

1.3 APPLICATIONS OF THE PROJECT

Draft Building Codes, New Zealand (2/DZ 4203,1989) & (2/DZ 4203/1, 1991) and Australian (DR 87163,1987), adopted the same gust factor for both flat terrain and complex terrain which assumes there is no difference in RMS velocity (turbulence) over the hill in each case. In fact, there are of course significant differences between the flat terrain and the complex terrain peak-gust speeds.

There are many structures which are vulnerable to the wind which are mounted on a hill site such as television masts, ratio antennas, building cladding. It is necessary to improve Building Codes as accurately as possible for the hilly terrain. This project was carried out with the purpose of investigating the effect of hills on the gust-speeds in the atmospheric boundary-layer in order to help the estimation of the effects

of hilly terrain on structural wind loads.

The data on the behaviour of the peak-gust speeds which was accumulated will also assist other applications such as wind energy, aviation and pollution in hilly terrain and will help the further understanding of wind characteristics on complex terrain.

1.4 Layout of Report

A description of the background theory for this experiment is given in Chapter 2.

Chapter 3 describes the experimental details of this project and the data is presented.

Chapter 4 discusses a comparison of the project results with the New Zealand Draft Building Codes (2/NZ 4203, 1989) and Australia Draft Building Codes (DR 87163, 1987).

Chapter 5 presents the conclusions to this project and references are listed at the end of the thesis.

Appendices include a table of turbulence intensity modifying factors and the Code rules for hills are listed.

CHAPTER 2

BACKGROUND THEORY

The basic cause of the natural wind is the difference in solar radiation at the poles and at the equator which produces temperature and pressure differences within the earth's atmosphere. These along with the effect of the earth's rotation, set up the wind circulation systems in the atmosphere. Due to an unsteady temperature gradient near the earth's surface from solar radiation and the effects of surface roughness, a turbulent boundary-layer in the wind flow is created. This discussion is restricted to strong wind and neutrally stable atmospheric conditions when mechanical turbulence dominates over convertive turbulence from surface heating. It is this condition which is of most concern to engineers involved in the prediction of damaging wind loads on structures.

2.1 THE ATMOSPHERIC BOUNDARY-LAYER

The boundary layer is the growing shear layer between a solid surface and an infinite stream, or the region of frictional influence. Its theory is well understood and the atmospheric boundary-layer has the characteristics which are conveniently summarized by Holmes (1986),

1. an increase of mean wind speed with height,
2. strong turbulent fluctuations of wind speed at all heights,
3. a broad band of frequencies of the fluctuations or gusts, and
4. similar patterns of gusts occur at all heights.

2.2 MEAN VELOCITY

The continually changing wind speed U(t) at a certain height Z may be averaged in the longitudinal direction over a length of time T_0, where T_0 is the record length which is large compared with the time scale of the fluctuations in U(t). The mean wind speed Vz can then be defined as

$$\overline{V}_z = \underset{T_0 \to \infty}{LIM} \frac{1}{T_0} \int_0^{T_0} U(t)\, dt \qquad 2.1$$

2.3 TURBULENCE

Turbulence is a 3D time-dependent motion in which vortex stretching causes velocity fluctuations to spread to all wavelengths between a minimum determined by viscous forces and a maximum determined by the boundary conditions of the flow. Turbulent flow is characterised by the existence of a time variant velocity superimposed upon an underlying steady 'time averaged' mean velocity component.

The fluctuations in wind velocity at a height Z are usually considered in terms of three orthogonal components u(t) parallel to, and v(t), w(t) normal to the mean flow direction, and in the longitudinal direction,

$$U(t) = \overline{V}_z + u(t) \qquad 2.2$$

The longitudinal component of the wind fluctuations contain most of the energy and is of most concern to the structural design. Consequently this discussion will be mostly confined to the wind flow behaviour in the longitudinal axis.

2.3.1 RMS Velocity

If the longitudinal velocity component U(t), is recorded over a period of time, T_0, which is the record length, then the mean square velocity in the longitudinal direction is expressed by

$$\overline{U^2(t)} = \lim_{T_0 \to \infty} \frac{1}{T_0} \int_{t=0}^{t=T_0} U^2(t)\, dt \qquad 2.3$$

Similarly:

$$\overline{u^2(t)} = \lim_{T_0 \to \infty} \frac{1}{T_0} \int_{t=0}^{t=T_0} u^2(t)\, dt = \sigma_u^2 \qquad 2.4$$

Where,

$$\sigma_u = \sqrt{\overline{u^2(t)}} = \textit{RMS velocity} \qquad 2.5$$

Similarly, we can get σ_v in the vertical direction and σ_w in the lateral direction.

σ_i is called the RMS velocity.

2.3.2 Turbulence Intensity

The RMS velocity is a very useful parameter to indicate the magnitudes of the fluctuating velocity components and the level of turbulent energy. However it is usually compared to the mean velocity to express the intensity independently of the wind speed.

The Turbulence Intensity is defined as

$$\textit{turbulence intensity} = \frac{\sigma_i}{\overline{V_z}} \qquad 2.6$$

It is recorded by ESDU (1974) that $\sigma_u \rangle \sigma_v \rangle \sigma_w$ in turbulent boundary-layers and for a surface roughness of Z_0 = 0.05m (open country), the turbulence intensities at 10m height would be $\sigma_u/\bar{V}_z$ = 0.21, $\sigma_v/\bar{V}_z$ = 0.15, and $\sigma_w/\bar{V}_z$ = 0.09 in atmospheric boundary-layers.

2.3.3 Reynolds Stresses

The Reynolds Stresses due to the momentum flux caused by the turbulence velocity fluctuations may be expressed by $-\rho\overline{uw}$ and another two components $\overline{uv}$ and $\overline{vw}$ which are usually quite small throughout the planetary layer and may be ignored. Teunissen (1970) suggests that the Reynolds stress which is determined by the variance ratios in the surface layer is a constant.

$$\frac{\overline{uw}}{\sigma_u \cdot \sigma_w} = -0.31 \qquad 2.7$$

ESDU (1974) recommend the value of $uw/(\sigma_u \cdot \sigma_w) = -0.285$ for the surface roughness length Z_0 = 0.05 m.

2.3.4 Wind Speed Power Spectra

Wind speed power spectra are used to describe the distribution of turbulent energy with frequency. If the contribution to the longitudinal variance in the range of frequencies from n to n+dn is given by $S_u(n)$, where $S_u(n)$ is called velocity power spectrum,

$$S_u(n) = \underset{\Delta n \to 0}{LIM} \frac{\overline{[u(t)^2]}_n^{\Delta n}}{\Delta n} \qquad 0<n<\infty \qquad 2.8$$

then the variance can be expressed as the total contribution from all frequencies,

$$\overline{u(t)^2} = \sigma_u^2 = \int_0^\infty S_u(n)\,dn \qquad 2.9$$

It is also often written in a non-dimensional form by plotting $nS_u(n)/\sigma^2_u$ against logarithmic frequency scale $\log(n/\overline{V})$.

2.4 FLOW OVER AN ISOLATED HILL

Because the hills can affect significantly the local variations in near surface wind speed, the fractional speed-up ΔS is introduced based at a given height above the local terrain. There are three characteristics of terrain whose spatial variation can cause variations in the near-surface wind field mentioned by Taylor and Lee(1984),

(1) surface roughness

(2) surface thermal and / or moisture properties

(3) surface elevation

The normalized wind speed (amplification factor) is defined as:

$$A(x,y,\Delta z) = \frac{U(x,y,\Delta z)}{U_0(\Delta z)} \qquad 2.10$$

where:

$$\Delta z = z - z_s(x,y) \qquad 2.11$$

is the vertical height above the local terrain.

$U_0(\Delta z)$ is the undisturbed or upstream wind profile

The velocity perturbation is defined as

$$\Delta U = U(x,y,\Delta z) - U_0(\Delta z) \qquad 2.13$$

So the 'fractional speed-up ratio' will be

$$\Delta S(x,y,\Delta z) = \frac{\Delta U(x,y,\Delta z)}{U_0(\Delta z)} = A-1 \qquad 2.14$$

The previous study of the wind flow over hills is useful summary of the velocity speed-up, roughness effects and turbulence over the hills. There are however, a number of alternative theoretical modelling studies of neutrally stable air flow over isolated hills being used.

The work of Jackson and Hunt (1975) which using the analytical theory rather than a numerical solution of various equation of motion to predict the wind flow over isolated hill is considered a milestone paper for estimating of 'speed-up' on hills. Their analysis suggests a simplified prediction method based on the equation,

$$\Delta S = k_t \cdot s \cdot \Phi \qquad 2.15$$

where,

ΔS is the fractional mean-wind speed-up.

K_t is the topographic type factor.

s is the position factor (s=1 at the ridge crest).

Φ is the effective upwind slope of the hill defined as $H/2L_e$.

H is the hill height.

L_e is the characteristic hill length or distance from the ridge to a level half the height below the crest in the direction of the wind.

The above parameters are shown in Fig.2.1.

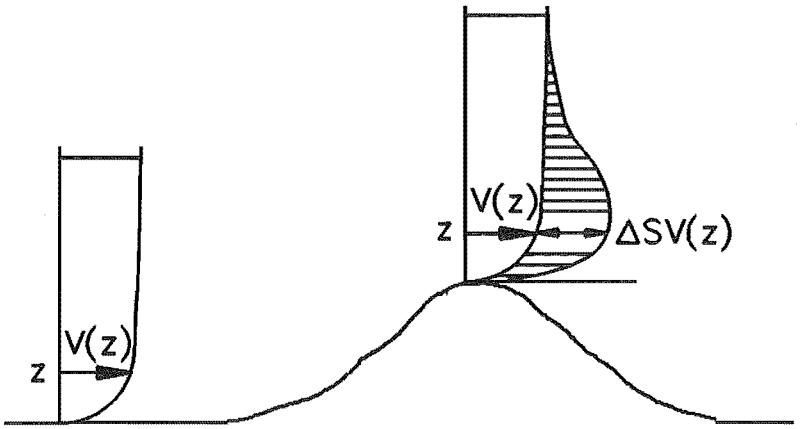

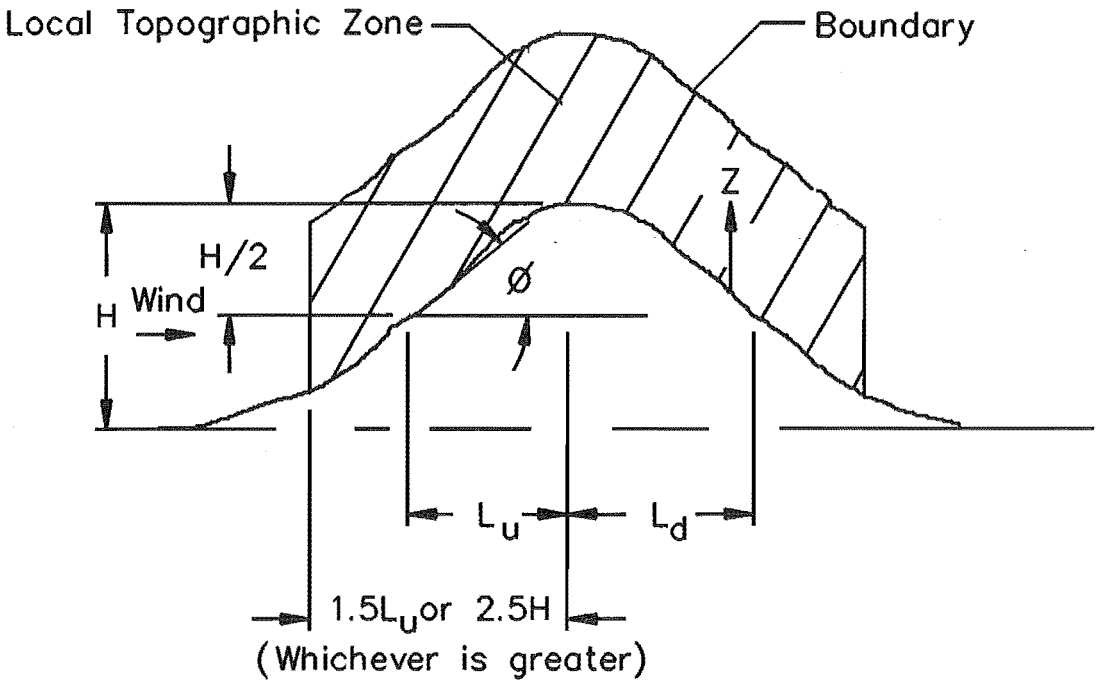

Fig. 2.1 Local Topographic Parameters.

The fractional speed-up equation from Jackson & Hunt is insensitive to the surface roughness and is determined by the pressure gradient well above the hill when the perturbation pressure and velocity is irrotational and independent of the boundary layer thickness.

The analysis is limited to low slope hills because of the assumption of the linearising effects from the hills and no flow separation.

The flow over the hill is divided into an inner and outer region with the perturbation velocities and pressures considered. (see Fig.2.2) Therefore arbitrary boundary conditions on the velocity and pressure are avoided.

The inner region in which significant changes in the Reynolds stresses (which determine the surface shear stress and velocity profile) associated with the hill would occur and affect the mean velocity. The height of the inner region l given by

$$\frac{l}{2L}\ln\frac{l}{z_0} = 2k^2 \qquad 2.16$$

Where k (=0.4) is the von Karman's constant.

In the outer region of irrotational flow the pressure gradient is set up by the hill and balanced by the inertial force which drives the inner layer.

Hunt(1973) and Townsend(1972) invoked the rapid distortion theory to estimate the turbulence changes in the outer region. They assumed the distortion to be sufficiently rapid so that an eddy has insufficient time to adjust to the local strain rate and to interact with other eddies while passing over the hill. The only effect on the turbulence from the distortion to the mean flow is to compress or lengthen and rotate individual vortex elements of the turbulence.

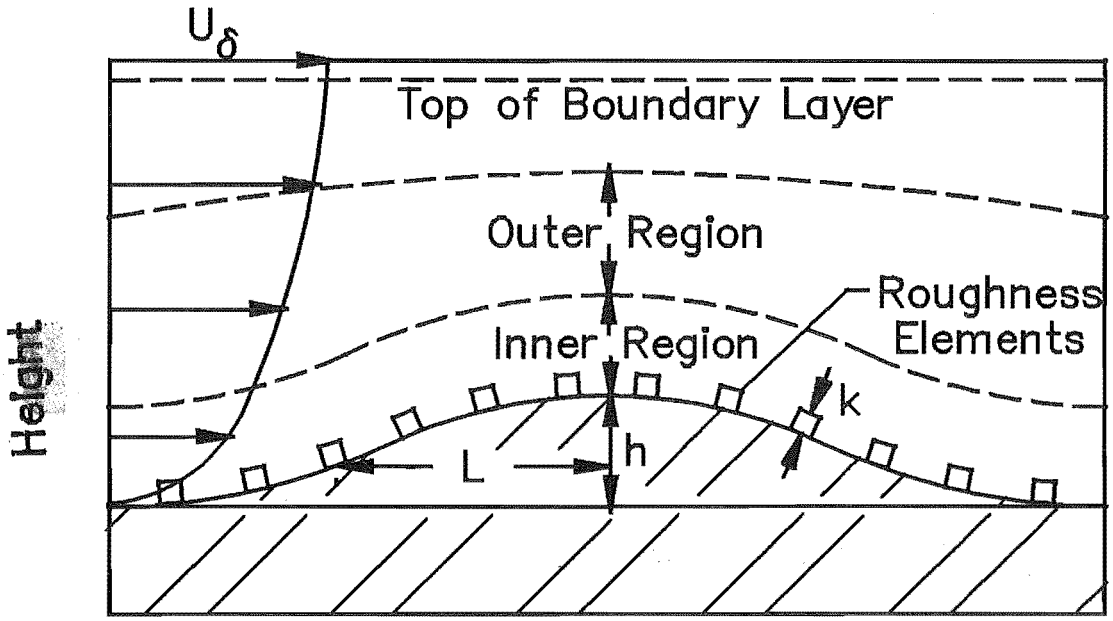

Fig. 2.2 Definition Sketch of Inner and Outer Regions.

For a symmetric hill (Askervein Hill), according to the rapid distortion theory, the longitudinal turbulent intensity will decrease and the lateral and vertical turbulent intensity will increase. Rapid distortion theory only predicts the changes of turbulence intensity in the outer layer.

Taylor and Lee (1984) developed the analytical theory from Jackson and Hunt and their own numerical analysis to produce 'simple guidelines for estimating wind speed variations due to small scale topographic features'.

As they stated that ΔS will usually be maximum at the surface but may decay significantly through the inner layer depending on the detailed shape of the terrain. The decay with height can be roughly estimated by the following equation,

$$\Delta S(0,0,\Delta z) = \Delta S(0,0,0)\, e^{-A\Delta z/L} \qquad 2.17$$

where,

A = 4 for 3D hills and A = 3 for the 2D hills.

L is the length scale of the hill which is defined as the distance from the ridge to a level half the height below the crest.

Δz is the vertical height above the local terrain.

The variation of the fractional speed-up ratio ΔS over the ridge which was verified against field and model by the Askervein Hill Project based on the above rules and has a simple form,

$$\Delta S = B \cdot \frac{h}{L} \cdot e^{-A(\Delta z/L)} \qquad 2.18$$

where

A = 3 and B =2.

Both the Draft Building Codes of New Zealand and Australia (2/DZ4203,1989, 2/DZ4203/1,1991 and DR87163,1987) use the

analytical theory suggested by Jackson and Hunt(1975) as in equation 2.15.

The values of K_t adopted by New Zealand and Australian Draft Building Codes have slightly modified values from each other and from those proposed by Taylor and Lee (1984). The values from those N.Z. Codes are listed below:

1.4 for escarpment (Aust. Code 1.6)

1.6 + 2.4 (L_u/L_d) with a maximum of 4.0 for 2D ridges, and 1.4 + 36 (Φ_d - 0.05) with a maximum of 3.2, for hills and ridges (Aust. Code, axisymmetric hills)

(Subscript u denotes upwind and d denotes downwind side of the hill.)

2.5 PEAK GUST SPEED

The experimental study of the variation of the mean-wind speed over smooth isolated hills has been fairly well performed as a part of the recent Askervein Hill Project. However there is no available data on the behaviour of the peak-gust speeds over complex terrain. Meanwhile, in the study of the wind loads on structures, the principal part is the estimation of the value of the extreme winds and the risk of their being exceeded. The gust speeds and average pressure coefficient are still being used for non-dynamic wind analysis for the wind load and they have also been used for this project.

2.5.1 Extreme Velocities From Experimental Data.

Mayne (1979) describes the accurate analysis of extreme winds from meteorological data. As the behaviour of the maximum (or minimum) gust speed of each recording describes the probability of occurrence of peak-gust speeds, it requires a large number of suitable meteorological data to obtain an accurate distribution of these extreme events.

(1) Distribution Functions

The distribution function is used to describe the probabilistic description of a variate.

PDF is the probability density function p(x) and CDF is the cumulative distribution function which is the integral function of the PDF, denoted by P(x), and is the probability that the variate is less than x,

$$P(x) = \int_{-\infty}^{x} p(x)\,dx = 1-\int_{x}^{\infty} p(x)\,dx \qquad 2.19$$

(2) Parent Distribution

The parent distribution of wind speed for meteorological data processing is a recording of continuous hourly-mean wind speed data over a long period of time and the form of the distribution determines the estimation of the extreme values.

When the wind velocity in the atmospheric boundary layer behaves in uncorrelated Gaussian fluctuations of mostly turbulent motions in orthogonal directions, the parent distribution could be expected as a Rayleigh distribution.

$$P(V) = 1-\exp(-V^2/2\sigma^2) \qquad 2.20$$

where:

P is the probability of a speed less than V.

σ is the standard deviation of V.

The Weibull distribution represents a whole family of distributions of which the Rayleigh form is only a special case when k=2.

$$P(V) = 1-\exp[-(cV)^{k}] \qquad 2.21$$

where:

P is the probability of a speed less than V.

c and k are constants.

As the different values of k describe the Weibull distribution, Davenport (1967) recommended the values of k ranging between 1.7 and 2.5.

(3) Type 1 Distribution

Many model distributions which are used in wind loading analysis are expressed by the equation

$$P_X(x) = 1-e^{-g(x)} \qquad 2.22$$

Where:

X is a variate of the parent distribution (taking on values x)

g(x) is a monotonic increasing function of x

Then, the extreme value distribution will be Type 1 :

$$P_Y(y) = \exp[-\exp(-a(y-U))] \qquad 2.23$$

Where:

1/a is the dispersion.

U is the mode.

Y is the largest of n values of Xi (taking on values, y, and $n \to \infty$)

(4) Fisher - Tippett (Type 1)

The Fisher - Tippett (Type 1) distribution accurately illustrates the behaviour of extreme winds in the well behaved

wind climates of temperate latitudes (ie: No tropical storm events,) and the extreme value distribution of annual maximum wind speeds will follow a Fisher - Tippett (Type 1) distribution. This adapts both to the distribution of maximum mean hourly and maximum gust speeds.

The CDF of the Fisher - Tippett (Type 1) distribution is given by

$$P(V)=\exp[-\exp(-y)] \qquad 2.24$$

$$y=a(V-U) \qquad 2.25$$

Where:

P(V) is the probability of a peak-gust speed less than V.
y is the reduced variate.
U is the mode of the distribution.
1/a is a scaling factor measuring the dispersion of the data.

The mean value of the distribution, μ, is given by:

$$\mu=U+(\gamma/a)=U+(0.5772157/a) \qquad 2.26$$

where γ is " Euler's constant ".
The variance is :

$$\sigma^2=\pi^2/6a^2=1.644934/a^2$$

So that

$$\sigma = 1.282550/a \qquad 2.27$$

The standard way of estimating these parameters is to average the peak-gust speed over a short period of time T_{av}, from each of a large number of independent recordings. (T_{av} can be obtained by combining consecutive data points). The

recording period T_0 should be sufficiently long to produce stationary data. This will be explained further in Chapter 3.

The analysis of a time history record of velocity fluctuations may be undertaken in a similar manner to obtain an estimate of the peak velocities during the recording.

The estimate for y is derived from rank m, where the extreme values are ranked by magnitude.

$$y=-\ln[-\ln(m/m_{max}+1))] \qquad 2.28$$

Then the extreme values could be plotted on the ordinate against the reduced variate y on the abscissa to produce the straight line in equation y = a (V - U) as shown in Fig.2.3.

This linear graph, y = a (V - U) will provide the values of U and 1/a in the appropriate units. This is achieved by fitting a straight line through the data points. The estimation of extreme value parameters should rest more on the central extremes and less on the largest and smallest values.
Therefore the expected mean peak gust speed and the variance may be calculated by using equations 2.27 and 2.28.

2.5.2 Theoretical Prediction of Peak Gusts

Davenport (1967) has analyzed the extreme-value distribution of the peak-gust speed in a one hour recording for wind loading applications.
If the parent distribution is the Weibull distribution, the extreme value distribution could be the Fisher-Tippett (Type 1) distribution, namely,

$$P\ (>V) = e^{-e^{-a(V-U)}} \qquad 2.29$$

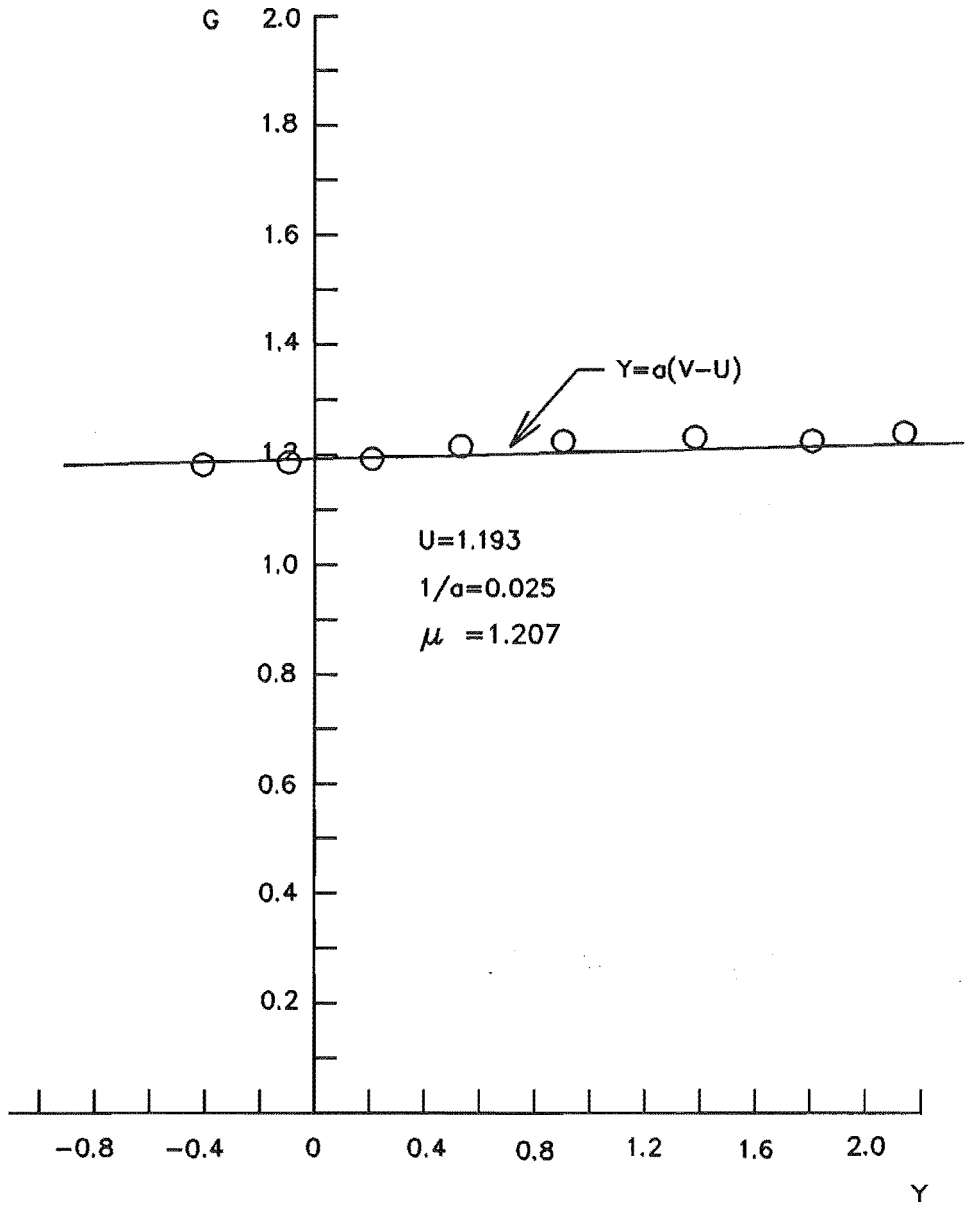

Fig. 2.3 An Example of Gumbel Plot for Fitting the Fisher-Tippett (Type 1) Distribution to the Extreme Data.

For the Rayleigh distribution, the dispersion 1/a and the mode of the distribution U will be,

$$1/a = \frac{\sigma}{\sqrt{2\log_e N}}$$

$$U = \sigma\sqrt{2\log_e N}$$

where N is the number of samples in each data set.

As the Fisher-Tippett (Type 1) distribution accurately represents the behaviour of extreme winds, an analysis of the extreme mean wind speed for structural design purposes was developed.

By using the extreme value analysis, Davenport (1964) related the mean peak gust speed to the mean wind speed by the following equations,

$$\hat{V} = \overline{V} + \hat{\eta}\sigma_v \qquad 2.30$$

where mean factor,

$$\hat{\eta} = (2\log_e \nu T_0)^{1/2} + \gamma(2\log_e \nu T_0)^{-1/2}$$

T_0 is the record length.
γ is the Eulers constant = 0.5772
υ is the measure of the average frequency of extreme gusts.

Considering the effect of the turbulence intensity, $\sigma/\overline{v}$ sample averaging time, T_{av} and the following record length, T_0, Mackey (1970) and ESDU(1972) suggested the relationship for the gust factor is,

$$G=1-A\log(T_{av}/T_0) \qquad 2.31$$

$$A=a(\sigma_v/\overline{V})^n$$

Mackey(1970) suggested that a = 0.6226 and n = 1.2716.

ESDU concluded that a = 2.4 and n = 1.33 but it was suggested that variations should be expected due to the different averaging times with respective field data being used.

Bowen (1979) developed a more simple relationship by measurements over an escarpment which may be justified in view of the extent of these variations in the measured peak gust values.

$$G=1+(\sigma_v/\overline{V})\log(T_0/T_{av}) \qquad 2.32$$

The commonly used empirical engineering relationship for the gust factor is

$$G = 1+g(\sigma_v/\overline{V}) \qquad 2.33$$

Deaves and Harris (1976) recommend the peak-factor g is 3.7 for T_{av} is 3 seconds, T_o equals 3600 seconds and this value of g is in common use by engineers.

Greenway (1979) described an analytical expression derived for the gust factors using the scaled mean wind speed to obtain a maximum gust speed. The gust factors are obtained as functions of the structural size and therefore can be used to obtain an appropriate design wind speed for any given structure.

It is confirmed by ESDU (72026) and others that the concept of a peak-gust speed averaged over a short time period, T_{av}, has severe limitations when applied to wind loading.

T_{av} can be related to the mean flow speed and the 'size' of a typical gust by Taylor's Hypothesis.

$$d_{gust} \propto T_{av} \cdot \overline{V}$$

Davenport pointed out that the important parameter affecting the response of the load on a structure to the buffeting of the turbulent eddies in the wind is the ratio of the typical structural dimension Dstr and the longitudinal integral length scale of the turbulence ${}^{x}L_{u}$.

Greenway (1979) then developed the use of the ratio $D_{str}/{}^{x}L_{u}$, and related gust factors directly to the structural size parameter D_{str}.

$$T_{av} = constant \; x \; D_{str}/\overline{V} \qquad 2.34$$

Where:

T_{av} is the averaging time

D_{str} is the structure or structural element of size

$\overline{V}$ is the mean velocity

Greenway's analysis is based on the horizontal wind spectrum having the Von Karman form, and the probability distribution of the horizontal wind velocity having the Gaussian form.

Through an empirical relationship giving the relevant averaging time for the measurement of extreme pressure loads on structures or structural elements of size D_{str}, Lawson (1976) has suggested the constant is around 4.5.

$$T_{av} = 4.5 D_{str}/\overline{V} \qquad 2.35$$

Analyzing in terms of the averaging time T_{av}, a formulation of gust factors based on 3-s average velocity is obtained by Greenway:

$$G = 1+3.25(\sigma_v/\bar{v})\,[1-8x10^{-5}(\bar{v}\,T_0/{}^{x}L_v)] \qquad 2.36$$

Where:

$\sigma_v/\bar{V}$ is the turbulence intensity of the wind.

$\bar{V}T_0/{}^{x}L_v$ is the number of turbulence length scales to blow over the structure during the observation time, T.

Most of the full-scale work on the effect of gust speeds on buildings and structures has been based on the idea of averaging wind speed over short time intervals. It has been explained by Greenway (1979):

(1) meteorology needs 2-5 s response time for its anemometers,
(2) Taylor's hypothesis, $T_{ed} \propto D_{ed}/\bar{V}$, where
T_{ed} is the time duration, D_{ed} is the eddy size
(3) for the experiment it is easy to average an electrical signal over fixed time intervals using a low pass filter.

From the above evidence, a 3 second average for the gust velocity recorded by a Dines anemograph seems reasonable, and is in fact, the averaging time adopted by the UK meteorological service to describe meteorological gust data taken from these particular instructions.

Using these historic data, the British wind loading code of practice (British Standards Institute Code of Practice, Wind Loads (1972)) recommends an averaging time of 3s for small structural elements such as cladding, roofing and glazing.

2.6 TOPOGRAPHIC MULTIPLIERS

In order to understand the effect on the wind speed by the

local topographical features such as hills, valleys and escarpments, topographic multipliers have been introduced by Both New Zealand and Australia Draft Building Codes.

Both Codes derive their topographic multipliers ($\bar{M}_t$ and $\hat{M}_t$) from fractional mean-wind speed-up estimates based on analytical theory which predicts for a simple isolated hill,

$$\Delta S = (\bar{V}_h - \bar{V}_0) / \bar{V}_0 = K_t \cdot S \cdot \Phi$$

Where: V_h is the local mean wind speed over the hill.
V_0 is the mean wind speed at the same height upstream of the hill over open, flat terrain at the reference position.

Both Codes use the same value of peak factor (g = 3.7) for the gust factor over the hill as well as over flat terrain.

It was shown in equation 2.33 that the peak-gust speed is simply related to the turbulence intensity, which is assumed to be the same as the hills and the flat terrain, also the RMS velocity has no change over the hill, so $(\sigma_v)_h = (\sigma_v)_0 = \sigma_v$.

Based on these assumptions, it follows that over flat terrain;

$$G_0 = \hat{V}_0 / \bar{V}_0 = 1 + 3.7 (\sigma_v / \bar{V})_0 \qquad 2.37$$

and similar over a hill,

$$G_h = \hat{V}_h / \bar{V}_h = 1 + 3.7 (\sigma_v / \bar{V})_h \qquad 2.38$$

It follows from equation 2.38 that

$$\bar{V}_h = \bar{V}_0 + \bar{V}_0 \cdot K_t \cdot S \cdot \phi$$

$$= \overline{V}_0(1+K_t \cdot S \cdot \phi) \qquad 2.39$$

$$\because \quad G_h = \hat{V}_h/\overline{V}_h = 1+3.7(\sigma_v/\overline{V})_h$$

$$\therefore \quad \hat{V}_h = \overline{V}_h(1+3.7(\sigma_v/\overline{V})_h)$$

$$= \overline{V}_h+3.7\sigma_v$$

$$= \overline{V}_0(1+K_t \cdot S \cdot \phi)+3.7\sigma_v$$

$$(\because \quad G_O = \hat{V}_0/\overline{V}_0 = 1+3.7(\sigma_v/\overline{V}_0), \quad \therefore \quad \hat{V}_0 = \overline{V}_0+3.7\sigma_v)$$

$$= K_t \cdot S \cdot \phi \cdot \overline{V}_0+\hat{V}_0$$

$$\hat{V}_h/\hat{V}_0 = 1+K_t \cdot S \cdot \phi \cdot (\overline{V}_0/\hat{V}_0) \qquad 2.40$$

$$\hat{M}_t = \hat{V}_h/\hat{V}_0 = 1+K_t \cdot S \cdot \phi/(1+3.7(\sigma_v/\overline{V})_0) = 1+\Delta S/G_0 \qquad 2.41$$

Equation 2.41 is utilised in the commentary section of both Codes to define the gust-speed topographic multiplier $\hat{M}_t$. Similarly, mean-wind speed topographic multiplier, is defined as

$$\overline{M}_t = \overline{V}_h/\overline{V}_0 \qquad 2.42$$

$$\because \quad \Delta S = (\overline{V}_h - \overline{V}_0)/\overline{V}_0 = K_t \cdot S \cdot \phi$$

$$\overline{V}_h/\overline{V}_0 = 1+K_t \cdot S \cdot \phi$$

$$\therefore \quad \overline{M}_t = 1+K_t \cdot S \cdot \phi = 1+\Delta S \qquad 2.43$$

Where the differences between $\hat{M}_t$ and $\overline{M}_t$ can be seen.

$\overline{M}_t$ is related to the fractional mean wind speed-up ΔS, for which full scale and some model data are already available from the literature of the Askervein Hill Project.

In order to compare the values of the Codes' gust-speed topographic multiplier $\hat{M}_t$, it may be related to the gust factors reported here by;

$$\hat{M}_t = \hat{V}_h/\hat{V}_0 = (\hat{V}_h/\overline{V}_h)(\overline{V}_h/\overline{V}_0)(\hat{V}_0/\overline{V}_0)$$

$$= G_h(1+\Delta S)/G_0 \qquad 2.44$$

It has been mentioned by the New Zealand and Australia Building Codes (NZS 4203, AS 1170) that

(1) the multipliers are presented for z=10 m,
(2) the effective slope of the hill is given by Φ_e and Φ_d,
(3) for intermediate values of Φ_e, use linear interpolation,
(4) A ridge or axisymmetric hill has a value of $H/2L_d$ greater than 0.05.

2.7 CONCLUSIONS

A brief description of relevant background theory from literature has been summarised above.

However, the accuracy of empirical equations remain largely unconfirmed due to the lack of model and full scale data but they do support in general the concept of this project.

The gust-speed topographic multiplier $\hat{M}_t$ has been developed and related to the gust factors, thus it may be closer to the definition.

The topographic multiplier $\hat{M}_t$ discussed in this project is the same as the profile multiplier, M_p, used in the latest New Zealand Draft Building Code (2/DZ/ 4203/1,1991). Where M_t is the maximum of the profile multiplier, M_p, the lee multiplier, M_l and the channelling multiplier, M_c.

CHAPTER 3

EXPERIMENTAL DETAILS

3.1 GENERAL INTRODUCTION

Askervein Hill <Fig.3.1> is located near the west coast of the island of South Uist in the Outer Hebrides of Scotland. Full details of the terrain are given by Taylor and Teunissen (1987). The hill has no abrupt features and is essentially elliptical in plan form with a major axis about 2 Km in length and a minor axis around 1 Km. Its maximum height above the flat, uniform terrain surrounding it on all but the eastern (downwind) side is 116m, with slopes dependant on the wind direction. The corresponding value of $H/2L_u = 0.26$ for the wind directions at 210° has been used for testing in the wind tunnel. The ground cover of the hill and surrounding terrain is mostly grass, low heather, low scrub and some flat, exposed rocks. This typical ground roughness for open farmland suggests an estimated surface roughness length, $Z_0 \approx 0.03$m. A 2m contour-interval map of the hill and nearby terrain is shown in Fig.3.2.

HT is the summit of the hill.

CP is the second reference position at the centre of the model called Centre Point.

BS is the base station which was established near the foot of the hill to assist in the field activities.

RS is the Reference Site located about 3Km to the SSW of the hill near Daliburgh which was used to make detailed full scale measurements of the undisturbed wind flow prior to its modification by the hill.

Most of the field and model tests had measurement positions set out along the 3 lines drawn through HT and CP known as A, AA and B as shown in Fig.3.2.

Fig. 3.1 Askervein Hill Viewed from West

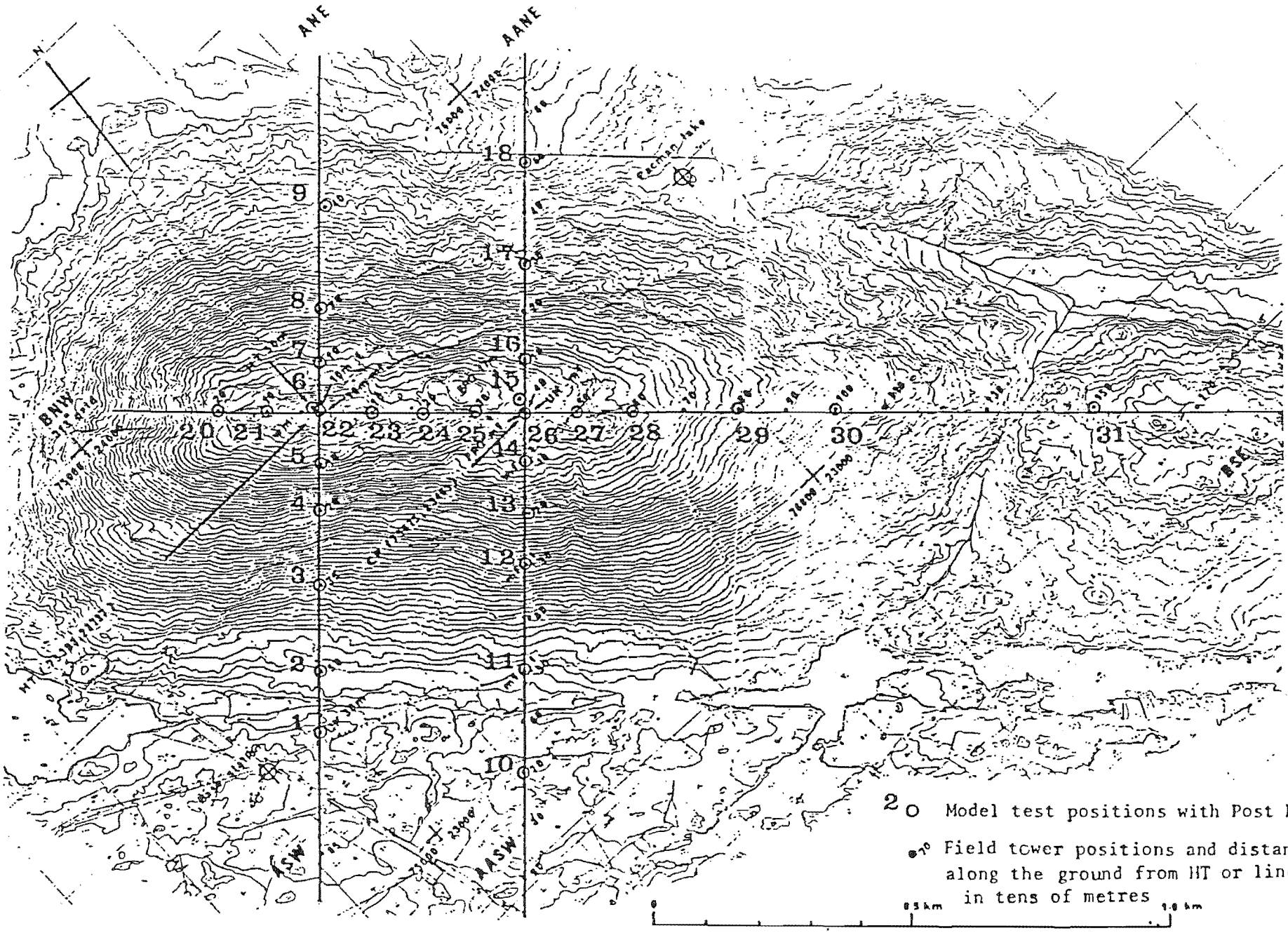

Fig. 3.2 High Resolution Contour Map of Askervein Hill.

The model and wind tunnel layout used in the current tests described here were the same as those utilised in the 1:2500 model tests reported by Bowen and Teunissen et al (1986) and Calvert and Bowen (1987). It was shown by Taylor et al (1987) that this model set up provided velocity and turbulence data over the hill which agreed well with those measured in the full scale tests. The results from this thesis therefore represent the full-scale situation during strong winds (neutral stability) and are complementary to the existing data gathered from the Askervein Hill Project.

3.2 INSTRUMENT LAYOUT

3.2.1 Wind Tunnel

The University of Canterbury boundary-layer wind tunnel in the Department of Mechanical Engineering shown in Fig.3.3a is an open-circuit tunnel with a 3:1 contraction ratio. It has a 12.2m long by 1.22m square working section as shown in Fig.3.3b which is fitted with an adjustable roof to reduce the small longitudinal pressure variations due to the presence of the growing boundary layer. It has two Woods 26kw contra-rotating fans with pneumatic blade-pitch control mounted down-stream of the test section which provides adjustable mean flow in the test section of 1 to 19m/s.

3.2.2 Askervein Hill Model

The wind-tunnel model of Askervein Hill used in these tests shown in Fig.3.4 was the same as that used by Taylor et al (1986). The model was built to an undistorted length scale of 1:2500 to suit the 1.22m working section of the University of Canterbury wind-tunnel. Its 1.122m diameter represented the same as a 2.80Km diameter circle in full scale about CP. The panels were painted and roughened with 14/25 grit sand (grain diameter 1.0 to 1.8mm) to match the required upstream floor

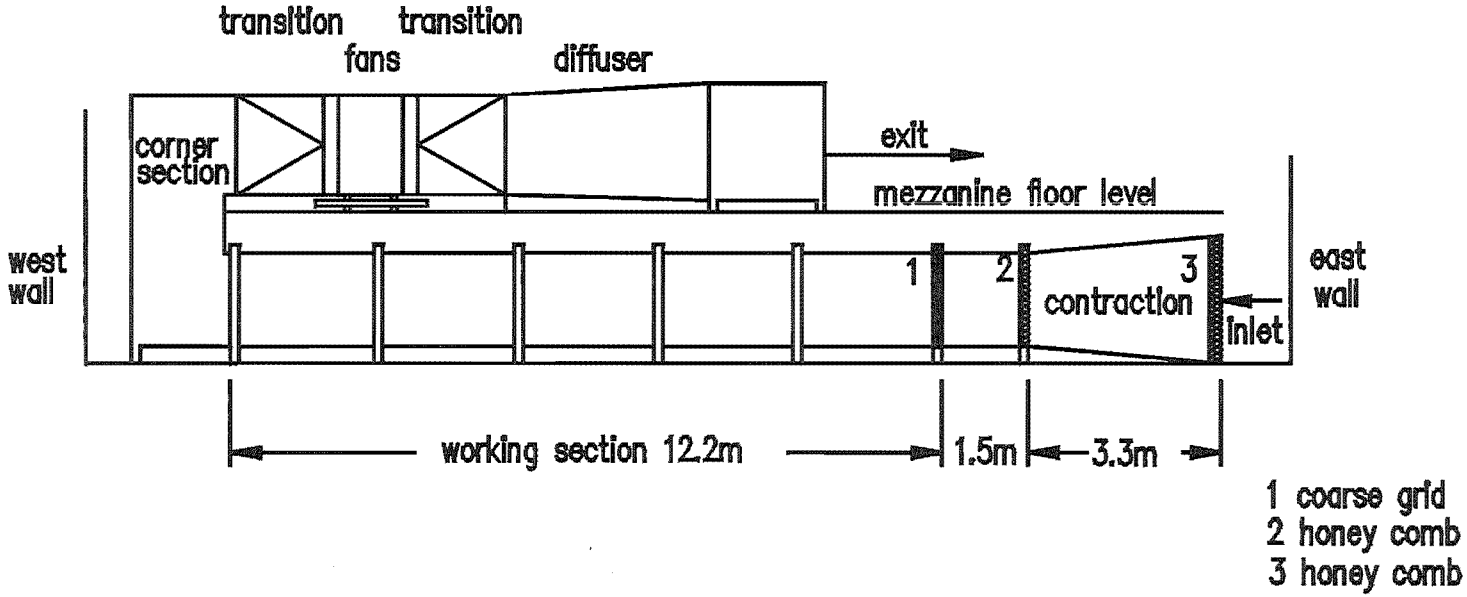

Fig. 3.3a. UNIVERSITY OF CANTERBURY BOUNDARY LAYER WIND TUNNEL

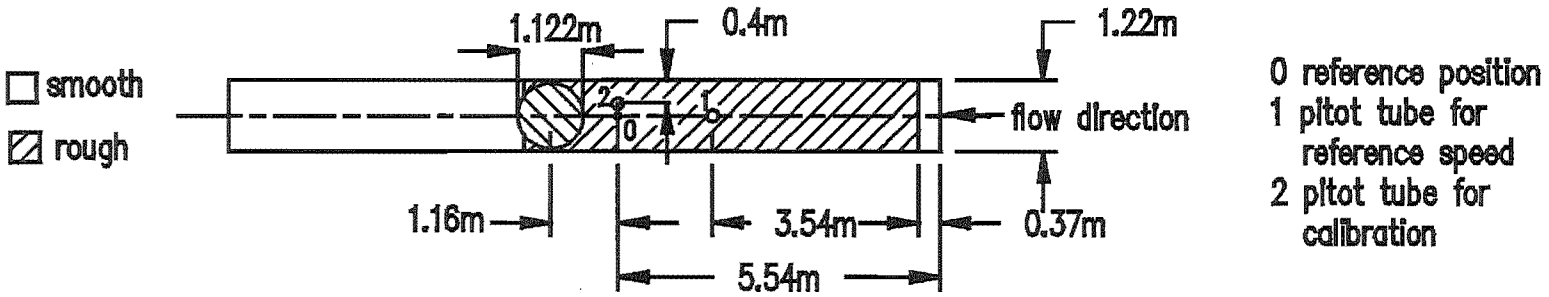

Fig. 3.3b. WIND TUNNEL WORKING SECTION LAYOUT

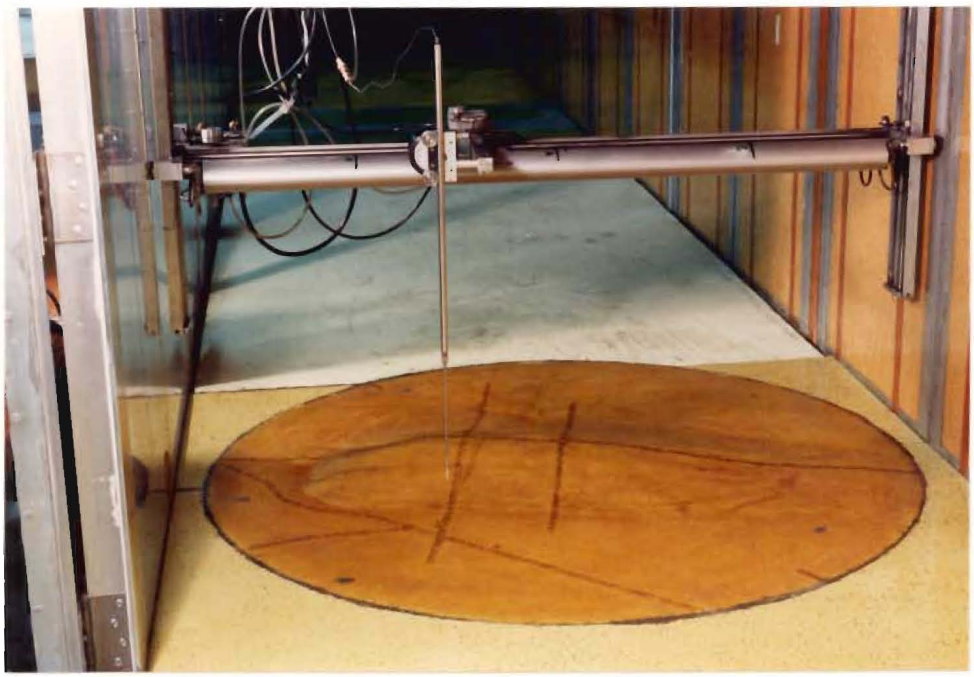

Fig. 3.4 Askervein Hill Model in Wind Tunnel.

roughness of the wind-tunnel. The overall height of the N.Z. model (whose full scale heighy above local ground level, H=116m) was about 47mm, or 118m in full scale, which is about 1.5% greater than the actual value. This slight distortion was assumed to have an insignificant effect on results obtained with model.

3.2.3 Equipment

A standard DISA constant-temperature hot-wire anemometer was used for the measurement of the velocities and turbulence in the wind tunnel. TYPE 55D01 constant temperature and TYPE 55D25 auxiliary unit were used as the basic anemometer unit. TYPE 55P14 single-wire horizontal probe was used as the velocity sensor which is sensitive to both longitudinal and vertical flow movement. A PDP11 mini-computer was used for acquiring the data, analysis and plotting. The diagram of the electronic system is shown in Fig.3.5. The height of the probe was automatically controlled by a program in a separate PC. The longitudinal position of the probe in the wind tunnel test section was controlled by the traverser control in two directions. Also a voltmeter and an oscilloscope were used as additional equipment to the experiment.

3.3 UPSTREAM REFERENCE CONDITIONS

3.3.1 Characteristics of Model Approach Flow

The reference position which was situated at a distance of 5.540 metres downstream of the entrance to the working section represents the flat terrain condition without any influence of the hill. In order to achieve reasonable approach flow similarity with the full scale tests, the wind tunnel was set up to match the previous tests by Calvert and Bowen (1987) which was reported in Taylor et al (1987) in the following neutrally-stable flow characteristic in Table 3.1:

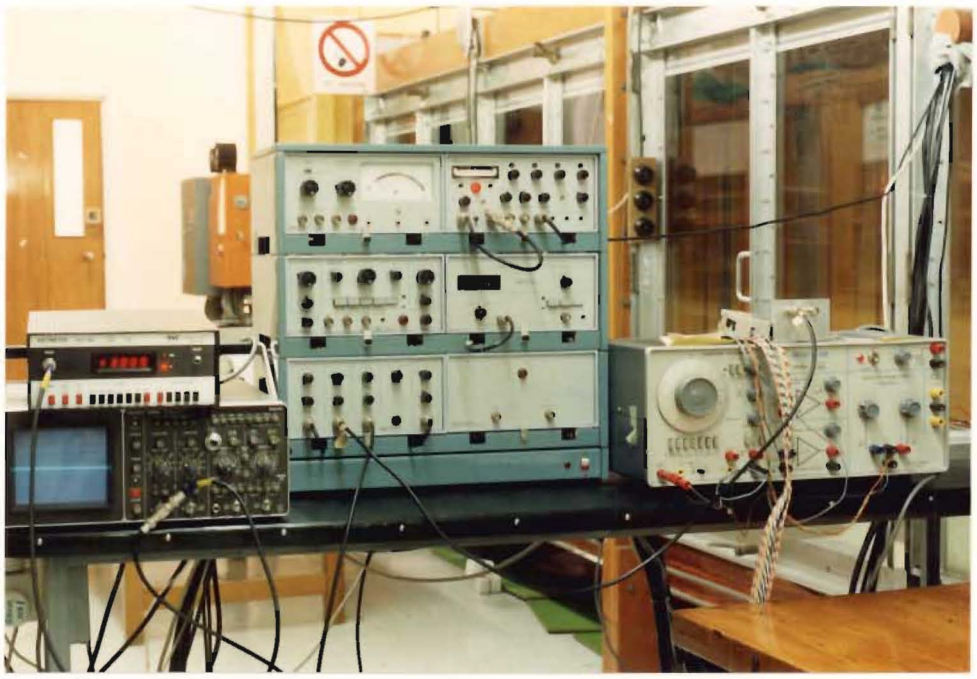

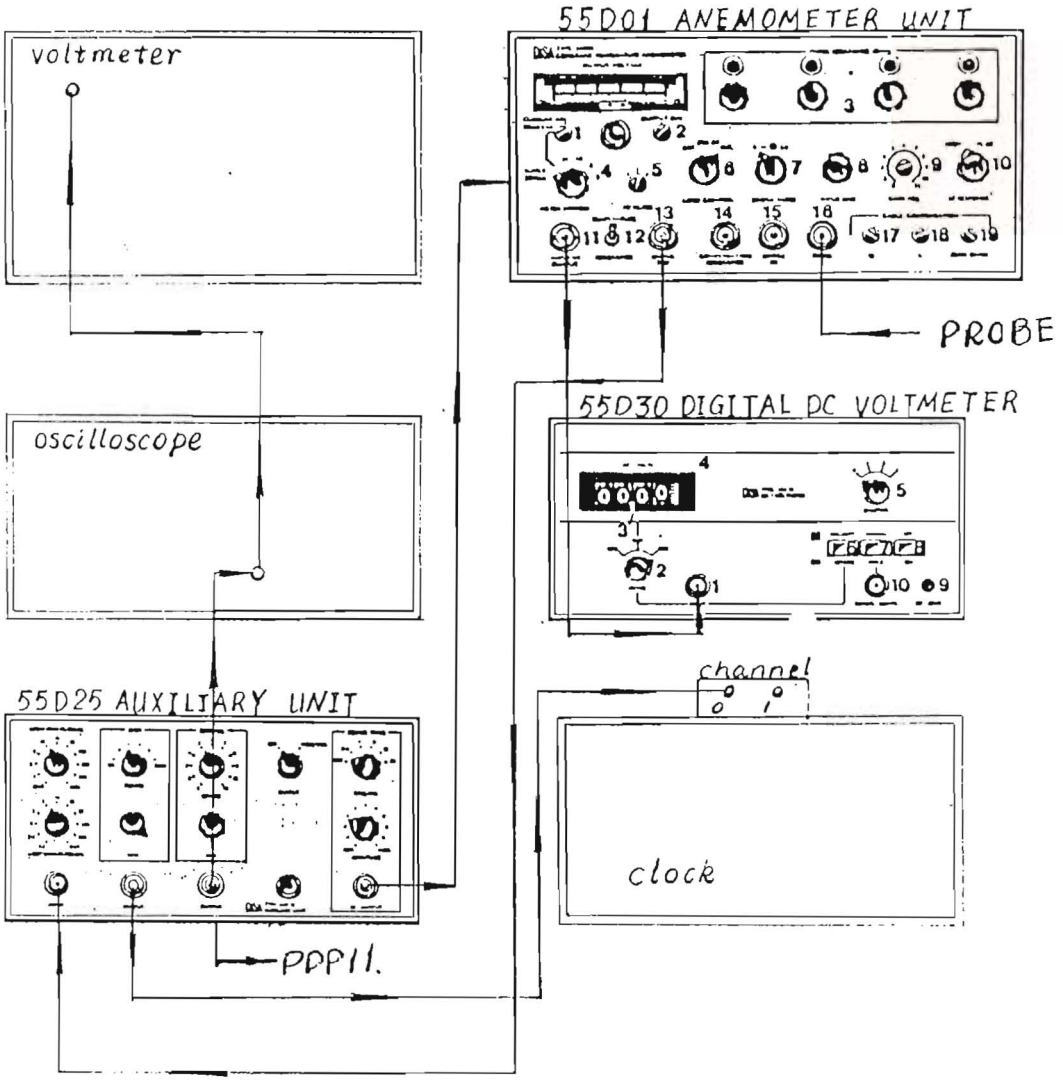

Fig. 3.5 Diagram of the Anemometer System

TABLE 3.1 SUMMARY OF CHARACTERISTICS OF MODEL AND PROTOTYPE APPROACH FLOWS EXPRESSED AS FULL-SCALE VALUES

	Standard * Characteristics	Askervein'83 Field Data^	Present Model
Geometric Scale	F.S.	F.S.	1:2500
Z_o	3cm	2cm	1.3cm
U_*Z_o/ν	~1400	778	0.23
U_*/U_r	0.04	-	0.036
U_{10}/U_r	0.58	-	0.59
$K_{10}=[U_*/U_{10}]^2$	0.0047	0.0041	0.0037
$C_g=[U_*/U_g]^2$	0.0016	-	0.0013
α	0.16	0.15	0.16
Z_δ	300m	-	275m
Re_δ	$3.6x10^5$	-	$1.8x10^5$
σ_u/U_* at 10m	~2.9	2.30	2.13
σ_u/U at 10m	~0.20	0.15	0.13

* Standard flow data taken mostly from ESDU (1974).

^ Turbulence characteristics taken from AES sonic anemometer data Run TU03-B, Taylor and Teunissen (1984).

The approach flows were considered reasonably adequate for the tests when compared with the neutrally-stable Askervein field data and the typical standard values taken from ESDU (1974).

3.3.2 Mean Velocity-Height and Turbulence Intensity Profiles

The mean velocity-height and turbulence intensity profiles of the approach flow at reference position are shown in Fig.3.6 and Fig.3.7 and were similar to the previous tests taken by Calvert and Bowen in 1987. Reference profiles were taken several times per day during the tests to obtain an accurate averaged upwind reference profile and to confirm the probe calibration accuracy in air flow temperatures that varied from 15-25°C. An indication of the accuracy of the profiles may be found in the limited spread of velocities at each height obtained between different reference velocity-profile data sets.

The longitudinal velocity power spectrum taken from the reference point at 10 metre height is shown in Fig.3.8 and is compared with the standard spectrum from ESDU (1974) for open country terrain at 10 metre height. Good agreement has been shown in Fig.3.8.

3.4 DATA ACQUISITION AND PROCESSING

3.4.1 Data Acquisition System

A proven data-acquisition system was used for the wind-tunnel tests. This system comprised the Hot-Wire calibration, data collection and plotting programs. A computer program was written and used for analyzing the velocity records and plotting the peak-gust data for this particular project.

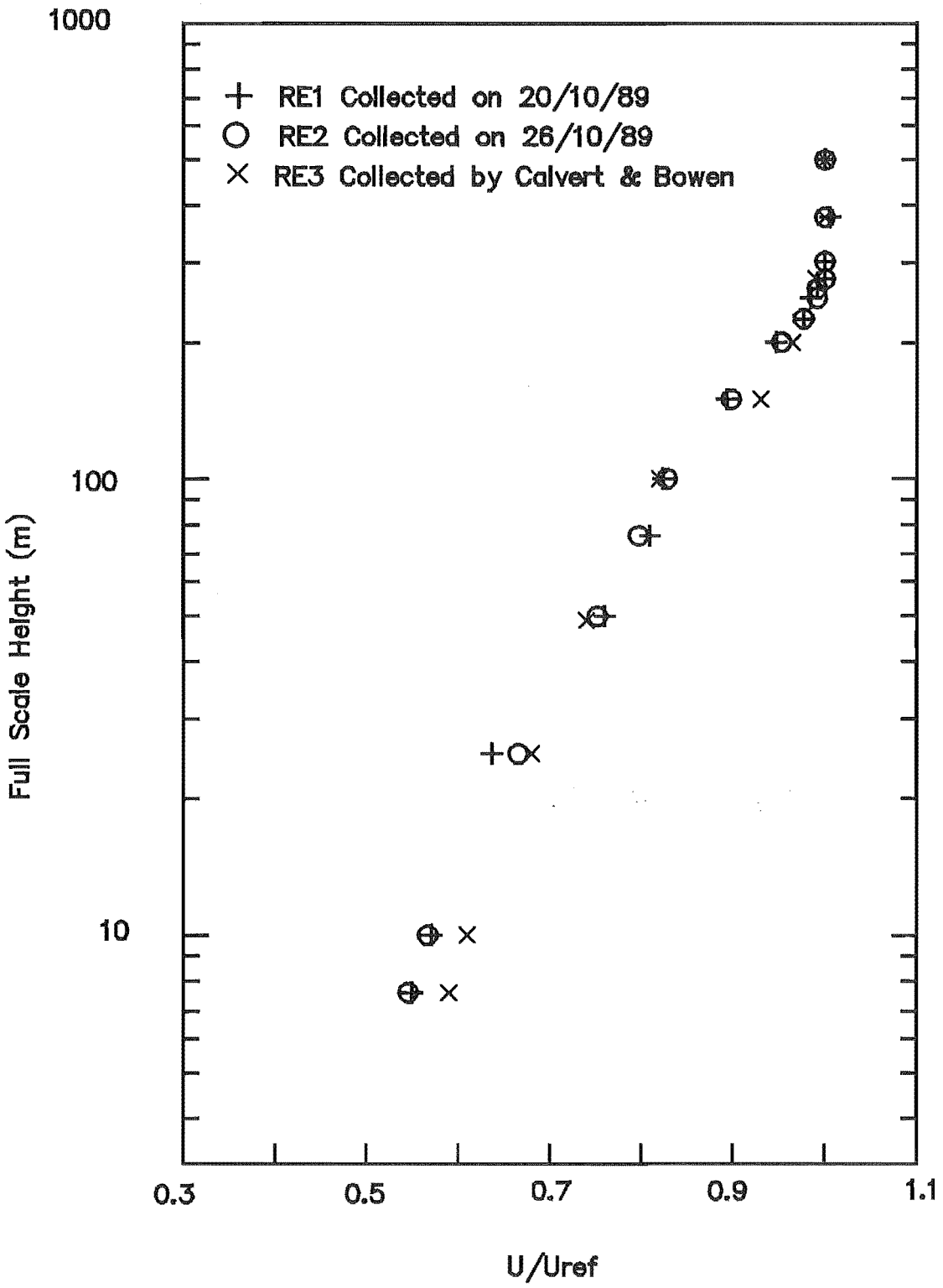

Fig. 3.6 Mean Velocity Profile at Reference Position.

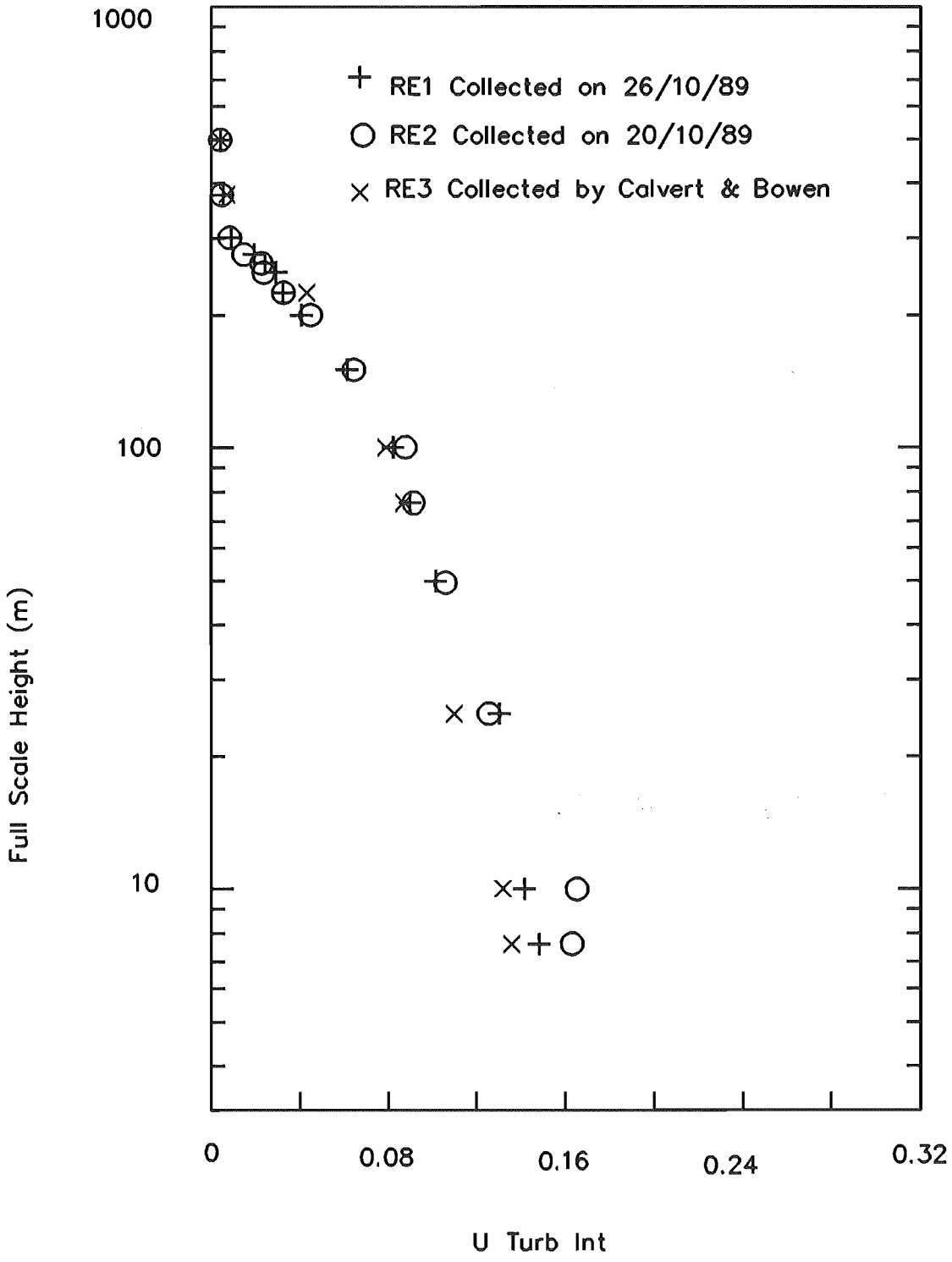

Fig. 3.7 Turbulence Intensity Profile at Reference Position.

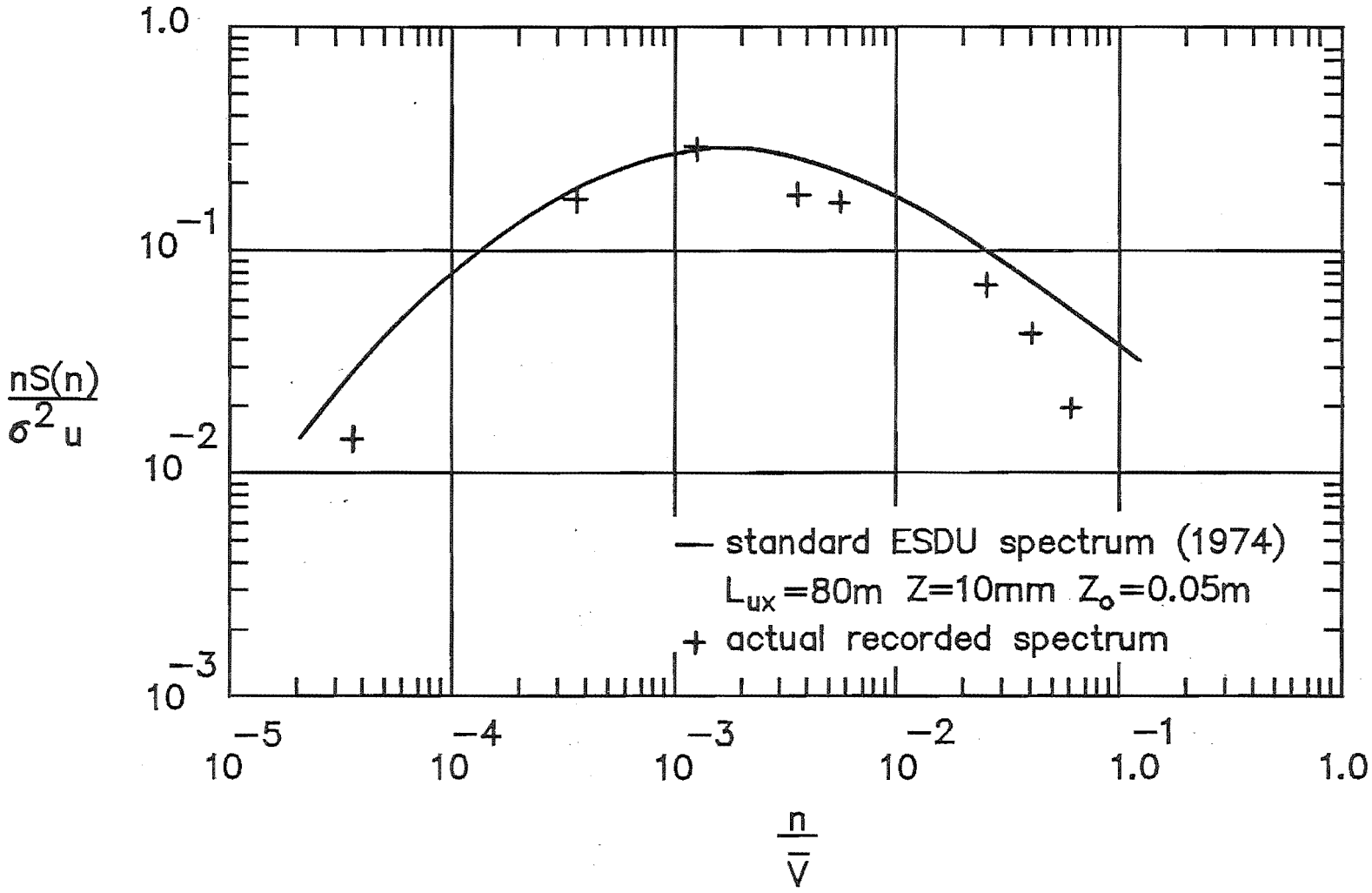

Fig. 3.8 Longitudinal Velocity Power Spectra at Reference Position.

3.4.2 Signal Generator

The data acquisition system was checked for accuracy by comparing the recorded data with a known sinusoidal input of a particular frequency from a signal generator.

A signal of 1KHz was generated by a signal generator and the signal sampled at a rate of 25KHz. The recorded profiles are given in Fig.3.9.

From the photos it may be seen that the signals are the same between the recorded computer and the input signal recorded on the oscilloscope. It was therefore considered that the data acquisition system is quite adequate for the wind-tunnel tests up to a sampling frequency of 25KHz.

3.4.3 Scan Rate

A very significant problem is that of selecting the best scan rate. When the scan rate is too fast, consecutive data will yield highly correlated and redundant data and will unnecessarily increase the labour and necessary computer memory for subsequent calculations, In contrast, if the scan rate is too low, it will cause aliasing with confusion between low and high frequency components of the original data. It was noted by Bendat & Piersol (1971) that the maximum frequency which can be defined by sampling at a scan rate of 1/T Hz is the Nuyquist frequency, 1/2T Hz.

3.4.4 Record Length

The record length is the length of time over which data is captured.

For this experiment the geometric scale of the Askervein Hill model was built as 1:2500. So if L_m is defined as the hill model size, Lf as the full-scale hill size, then, the length scale is the rates of hill model size / full-scale hill size = L_m / L_f = 1/2500.

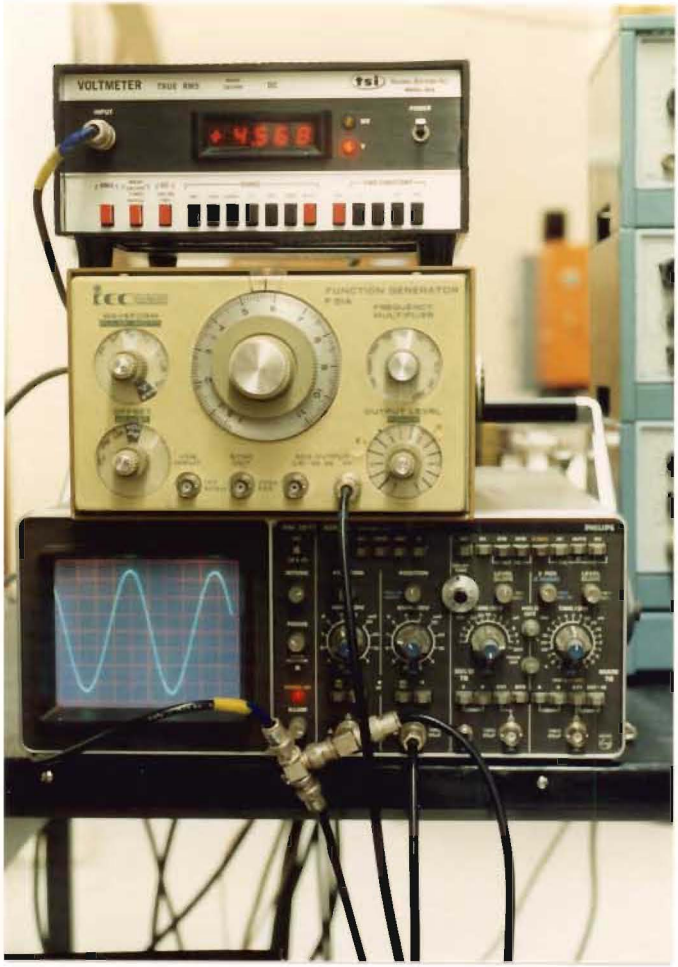

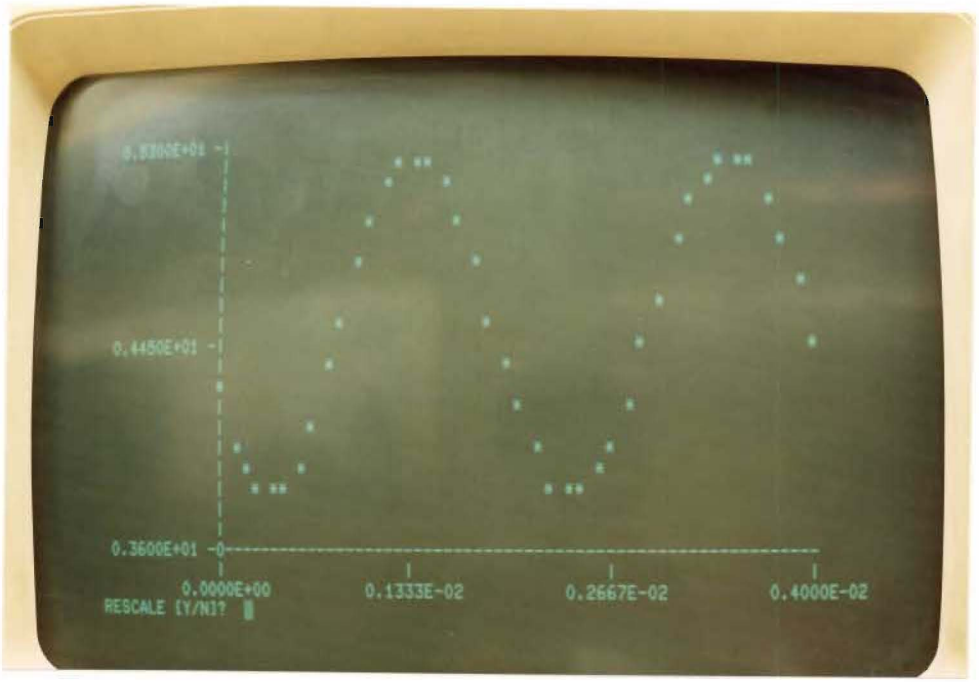

Fig. 3.9 Comparison Generated and Known Data.

The velocity for typical strong winds at 10 metres height could be conveniently taken as 30 m/s (full scale). So if U_{10} is defined as the speed in the wind-tunnel proportional to the wind speed at 10 metres height in full-scale and U_r is the wind-tunnel operating speed equals to 13m/s. U_f is defined as the full-scale speed at 10 metres height. According to the approach flow characteristics in Table 3.1, $U_{10}/U_r = 0.59$. So, when U_r=13m/s, U_{10}=7.5 m/s. Then the velocity scale becomes $U_{10} / U_f = 7.5m/s / 30m/s = 0.25$.

If T_m is defined as the averaging time for the model in the wind-tunnel and T_f as the averaging time for the full-scale. So the time scale for this experiment is $T_m / T_f = L_m/L_f \times U_f/U_{10} = 1/2500 \times 1/0.25 = 1/625$.

The equivalent model record length for one hour's full-scale recording is 3600/625 = 5.76 seconds and 0.96s for a 10 minutes F.S. recording. The shortest record length in full-scale for a stable average velocity is normally considered to be about 10 minutes. Flay (1978) and ESDU (1972) suggests that the record length between 30 minutes and one hour would produce stationary data. ESDU (1972) states that for record length (T_0) less than 45 minutes, the maximum T-second wind speed occurring in a particular period will generally decrease as the record length decreases.

The original model data recorded was limited by the computer memory to 48 blocks of 1024 samples (49,152 samples) taken at a sample rate of 5 KHz. So the record length of each data set for model scale is 48x1024/5000 = 9.830 seconds and for the full scale becomes 9.830 x 625 = 1.707 hours. It is long enough to divide into 8 independent sub-records of 6 consecutive blocks (6144 samples), each of which represents an adequate 12.8 minutes in full scale record length.

3.4.5 Sampling Frequency

The necessary sampling frequency is therefore determined by the highest frequencies in the signal. This in turn is

determined by the frequency response of the sensor itself. So, in order to select the sampling frequency it is very important to determine the maximum frequency of interest in the signal. The sampling frequency is required to be at least twice the highest frequency component in the signal to avoid aliasing.

If the full scale frequency is greater than 2-4 Hz then the signal has very little energy and is of little interest to engineers. Using the time scale of 1/625 developed in section 3.4.4, the equivalent upper frequency limit in the model tests is 2.5KHz. A sampling frequency of 5 KHz was therefore chosen for this experiment.

3.4.6 Filter

A low-pass filter was used for eliminating the high frequency noise from the incoming anemometer signal. The 55D25 incorporates an amplifier, and the amplifier could introduce a slight amount of additional noise in cases where the noise level out of the anemometer is very low. Because the low-pass filter in the DISA 55D25 auxiliary unit has a half-power point of 2 KHz, so the incoming data was filtered at 2 KHz. Aliasing could therefore be minimized by filtering which removes all frequencies greater than 2 KHz.

3.5 THE WIND-TUNNEL MODEL TESTS

3.5.1 Hot Wire Calibration

The single horizontal DISA hot-wire probe was calibrated against a nearby pitot tube which was shown in Fig.3.3b. The hot-wire probe was situated 400mm (free stream) above the rough surface at reference position in the wind-tunnel. The pitot tube was located at the same height and at the same Y direction of the hot wire, 400 mm away the wall of the wind tunnel to avoid the influence of the wall. Because the differences in calibration could result in the most significant errors in the tests, suitable measures were adopted in the hot wire

calibration to keep these errors to minimum. Long term calibration drifts were
eliminated by frequent recalibration (daily) of the probe and by cleaning the probe with alcohol before each calibration. Measurement differences between profiles were further reduced by normalizing each profile to the reference velocity and checking the zero-flow output voltage before each profile. As the time of the measurement of a single profile would only take 20-30 minutes, the calibration drift was considered negligible during the calibration period.

3.5.2 Reference Speed

The reference speed was monitored by a pitot static tube located well above the boundary-layer, and 1.63 m in front of the reference position. Small variations in mean wind-speed were eliminated by measuring a reference mean wind-tunnel speed simultaneously with every speed measurement in the boundary-layer flow and subsequently normalizing all results to a single value of reference speed taken as 12.7 m/s.

3.5.3 Wind Direction

The model was tested at a single wind direction of 210° in the boundary-layer of the wind-tunnel. This direction was chosen as it represented the direction for which the most data was obtained in the field tests. It is also the direction given the most attention by earlier model tests.

TABLE 3.2 FULL SCALE HILL SHAPE CHARACTERISTICS FOR THE WIND DIRECTIONS TESTED

Test wind direction	Length scale of hill L	H/L	L/Z_0
210°	200	0.58	6.7×10^2

H (= 116m) is the hill height at HT above surrounding flat land.

Z_0 (= 0.03m) is the full scale roughness length.

3.5.4 Measurement Positions and Heights

In order to get a clear picture of the hill flow, the test positions were selected in the following positions along line A as shown in Fig 3.10.

Measurement Positions:

- Reference position 0
- Position 2
- Position 4
- Position 5
- Top of the hill,position 6
- Position 7
- Position 8
- Position 9

The measurement heights adopted for the present tests were limited to those shown in Table 3.3.

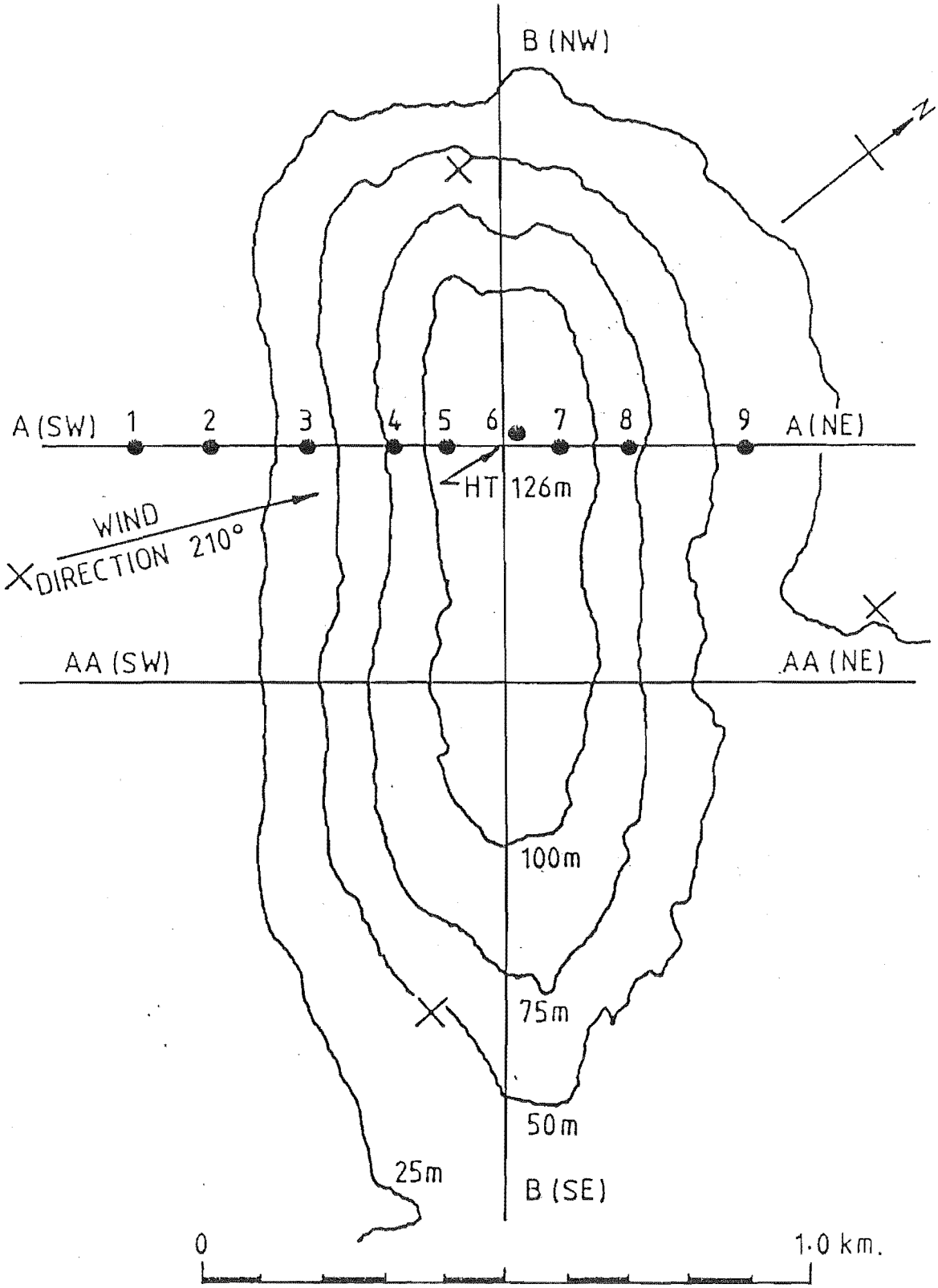

Fig. 3.10 Contour Map of Askervein Hill Showing Measure Positions and Wind Direction of the Model Tests.

TABLE 3.3 THE HEIGHT OF THE MEASUREMENT

Full Scale Height (m)	Model Scale Height (mm)
10	4
116 (height of the hill)	46.4
232 (2 * hill height)	92.8
348 (3 * hill height)	139.2

3.6 PRESENTATION OF THE TEST DATA

In order to understand the behaviour of the peak-gust wind speeds over a hill, raw data was captured as described earlier. At each measurement position, the data recording was divided into 8 independent records of equal length, each representing just over 12.8 minutes in the full scale.(see section 3.4.4). The peak-gust speed in each of the 8 records were ranked and plotted in terms of the reduced variate Y to obtain the mean peak-gust speed at that location. Using the same raw data, consecutive data points were then combined and averaged to obtain a range of full-scale averaging times from 0.125 seconds to 24 seconds (see Table 3.4) and the peak-gust analysis was repeated for each new averaging time. The RMS. velocity, peak velocity, mean velocity, the data group, gust factor, the ranking of the gust factor M and the reduced variate Y were also obtained for each averaging time.

Model Sampling Frequency, f = 5000 Hz.
Full Scale Sampling Frequency, f = 8 Hz.

TABLE 3.4 AVERAGING TIME

Recorded Data	Full Scale Averaging Time
original data	0.125 s
combine 3 adjacent data points	0.375 s
combine 2 further adjacent data points	0.75 s
combine 2 further adjacent data points	1.5 s
combine 2 further adjacent data points	3.0 s
combine 2 further adjacent data points	6.0 s
combine 2 further adjacent data points	12.0 s
combine 2 further adjacent data points	24.0 s

3.6.1 Mean Velocity Profiles

The variations of the mean flow velocities over the Askervein Hill model at the different heights are presented in Fig.3.11.

The comparisons between model predictions and sample normalized wind speed has been well illustrated and discussed by Salmon et al (1987).

From Fig.3.11 we can see the mean velocity decreases from

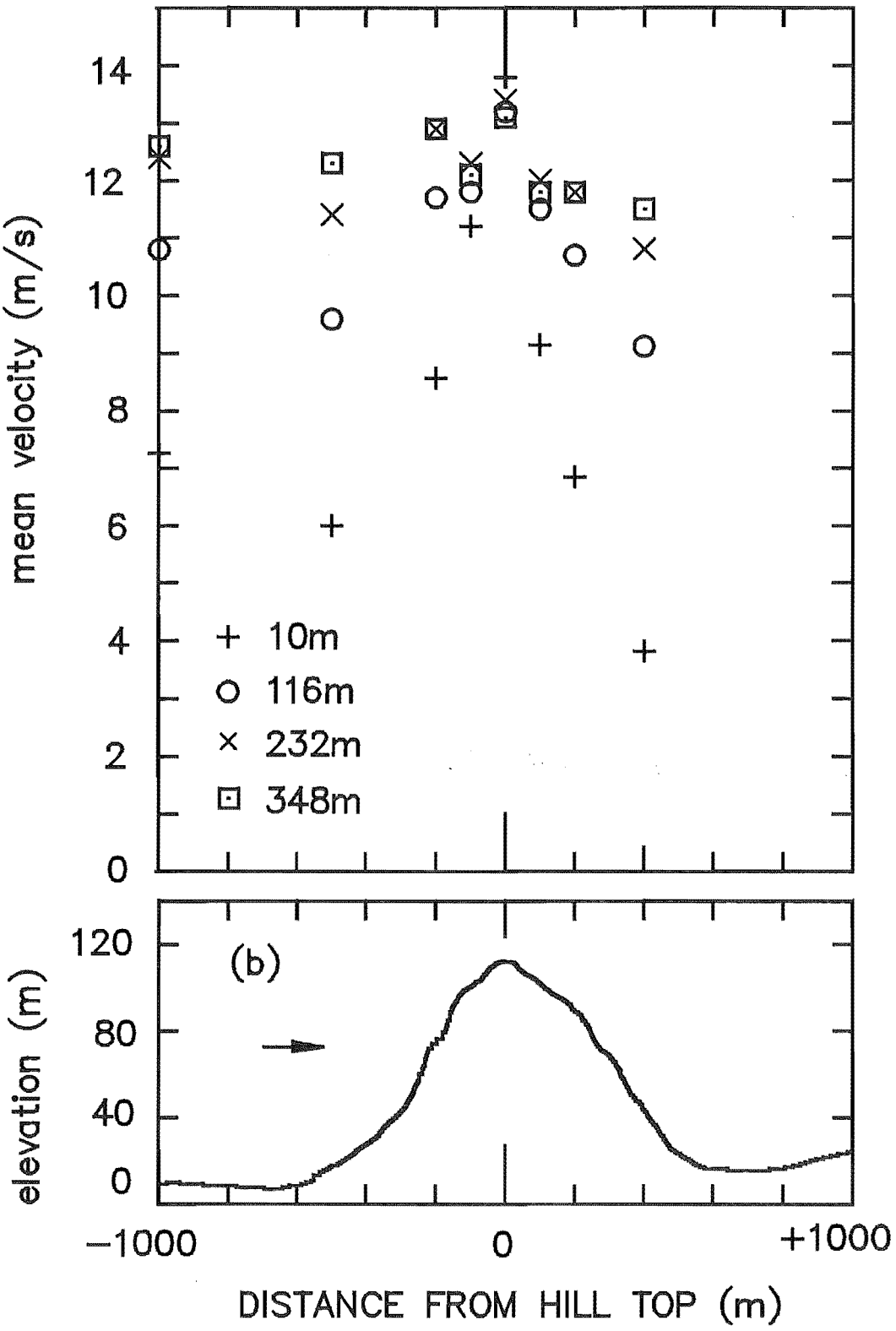

Fig. 3.11 Mean Velocity Variations over Askervein Hill at Four Different Heights above Local Ground Level.

the reference position until the upwind side of the hill, then it largely increases toward to the ridge. After the ridge, the mean velocity decreases along the downwind side of the hill. It also shows that the scale of the mean velocity variation decreases as the height of the measurement goes up, which indicates less influence from the hill. Good agreement has been found between the previous data provided by Calvert and Bowen (1987) and these tests.

NB. Note that for all figures showing data over the hill, the data for the reference position is plotted at the left hand edge of the figures. The heights chosen represent 10 metres,1, 2, and 3 hill heights.

3.6.2 Mean RMS Velocity Profiles

The variations of the RMS velocity profiles over the isolated hill model at four different heights are shown in Fig.3.12. This figure displays the RMS velocity decreasing in the upstream until the ridge but a steep rise occurring at the lee of the hill at low height (10m) indicating possible separation.

3.6.3 Turbulence Intensity Profiles

Turbulence Intensity Profiles in Fig.3.13 represent the variation of the turbulence intensity at four different heights over the hill.

It reveals the turbulence intensity at its lowest value over the ridge which is a welcome characteristic for design engineers.

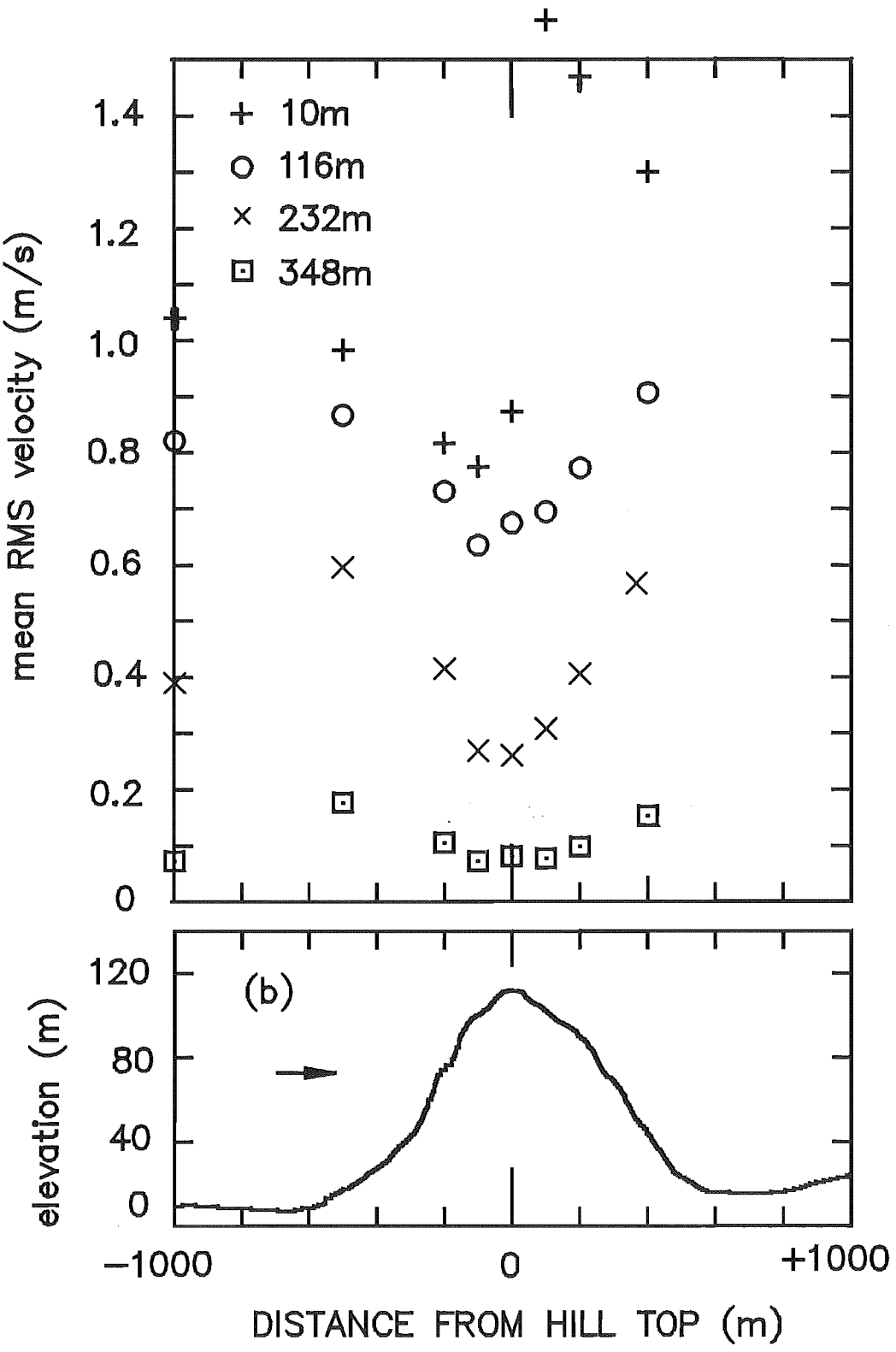

Fig. 4.12 Variation of the RMS Velocity over the Askervein Hill Model.

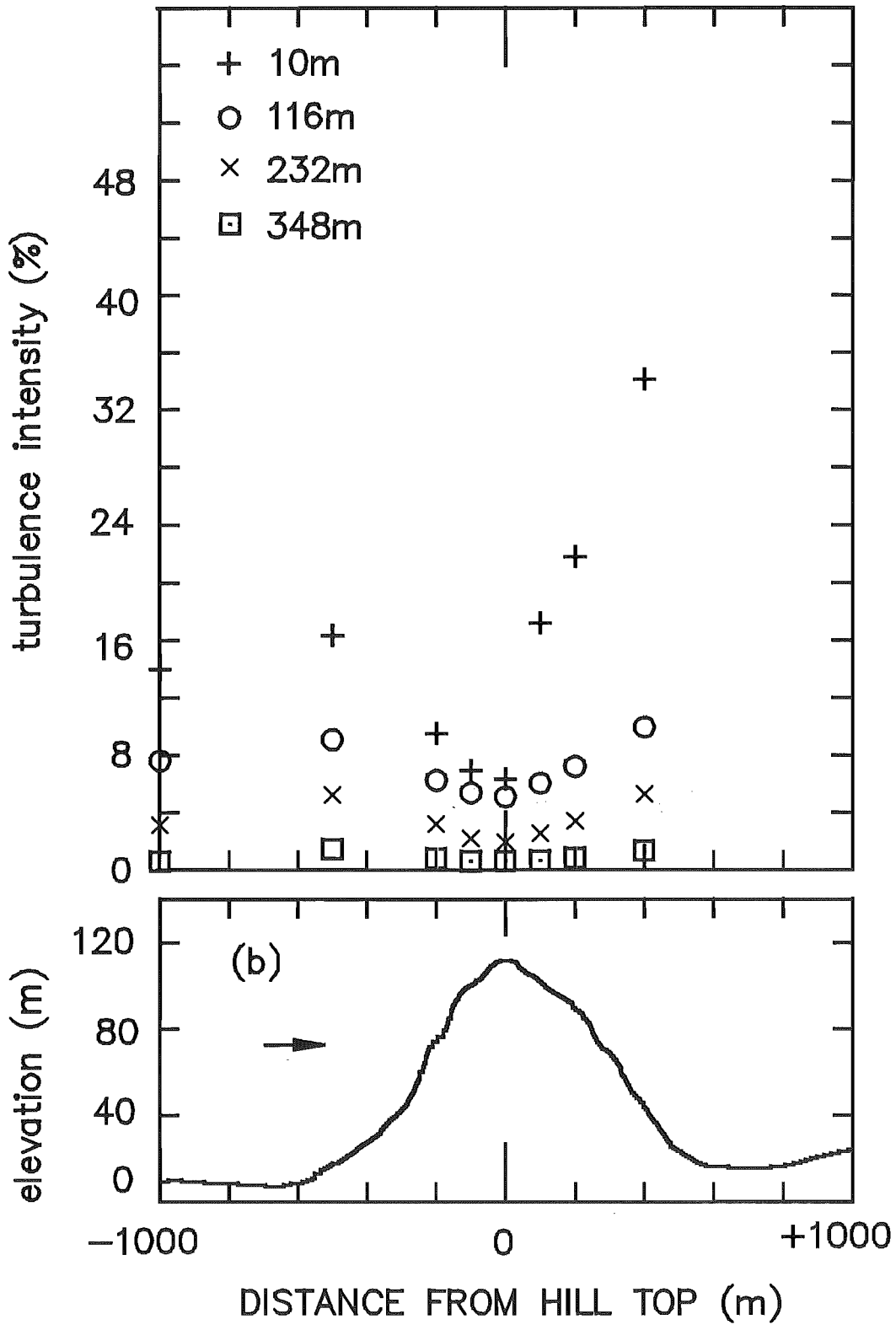

Fig. 4.13 Variation of Turbulence Intensities over Askervein Hill Model at Four Different Heights above Local Ground Level.

3.6.4 Peak Gust Factors

The variation of peak gust factors over the isolated hill model at full-scale averaging time of T_{av}=3 seconds at four different heights is shown in Fig.3.14. The gust factors at 10m height over different averaging times are shown in Fig.3.15. A full discussion about the influence by the hill to the gust factor is provided in Chapter 4.

3.7 CONCLUSIONS

The experiment was successfully set up to match the previous tests by B. Calvert and A.J. Bowen for providing an extensive, reliable and generally replicable set of velocity data at four heights above the hill.

Profiles of mean velocity, RMS velocity, turbulence intensity and gust factors over the Askervein Hill have been presented. Although there are a few possibilities of anomalies, the data is in general considered to be able to show reliably the changes in the flow structure as it passes over the hill.

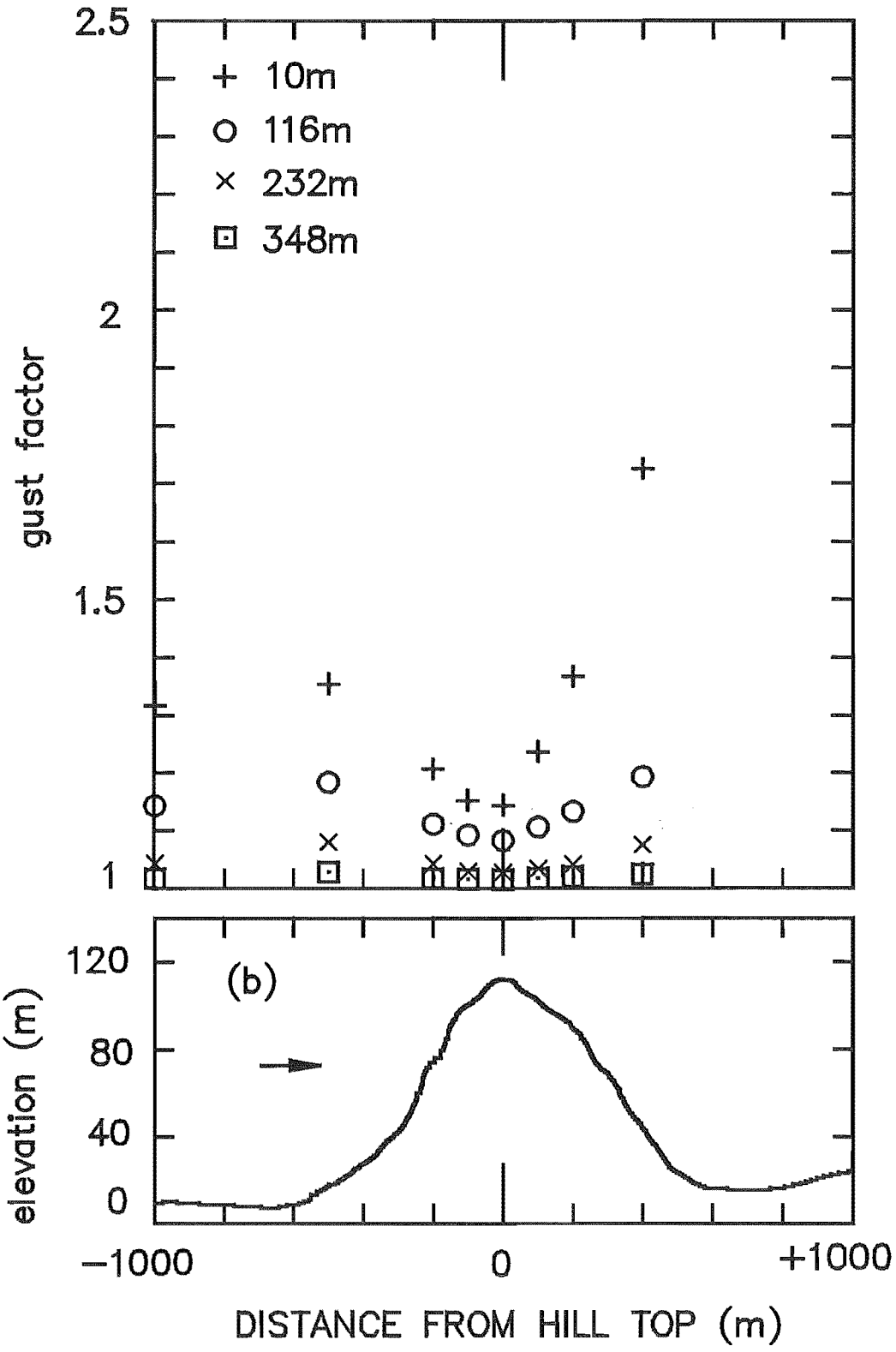

Fig. 3.14 Variation of Gust Factors over the Askervein Hill Model at Four Different Heights above Local Ground Level.

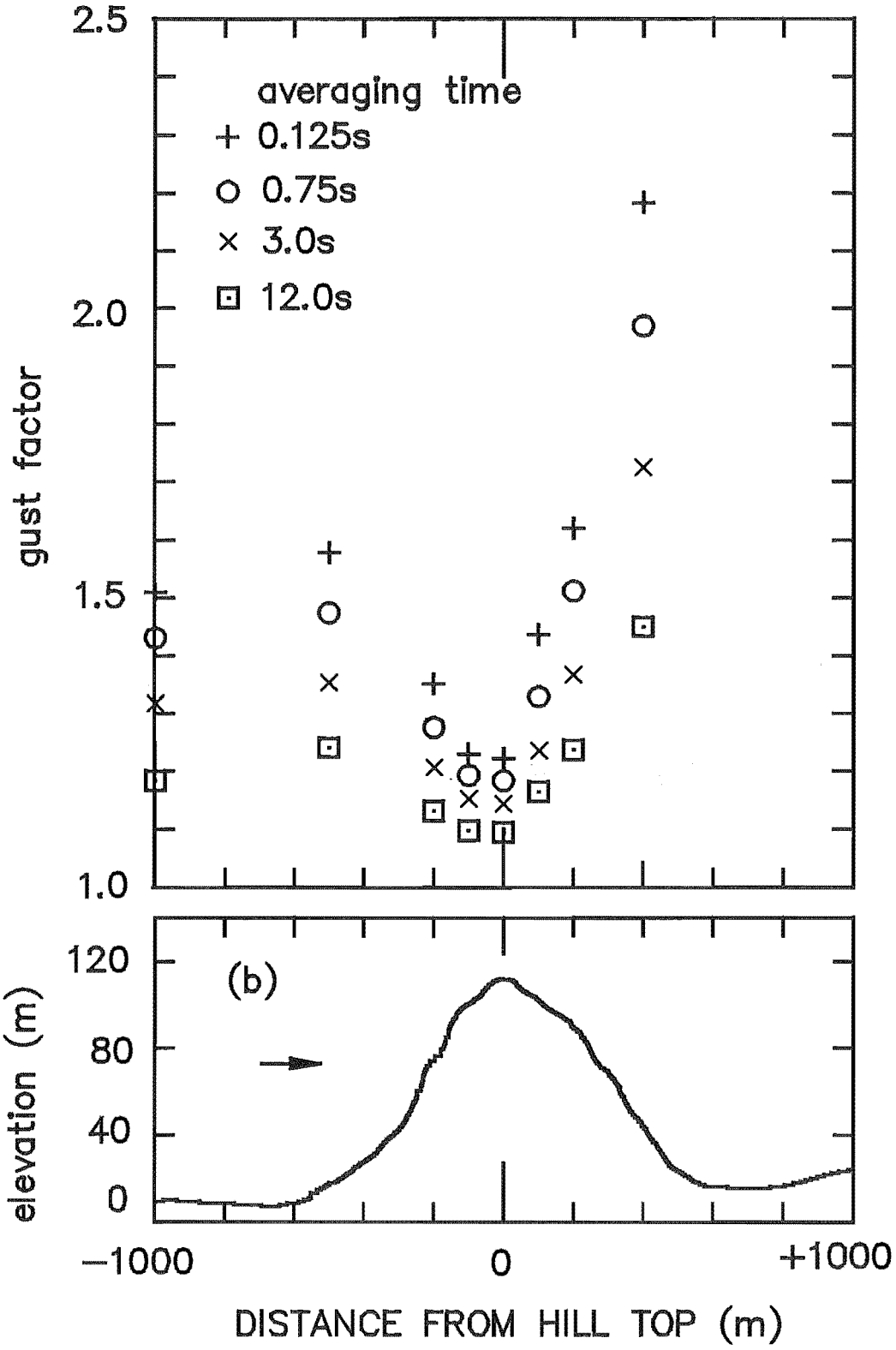

Fig. 3.15 Variation of Gust Factors over the Askervein Hill Model at Different Averaging Times. (HEIGHT=10m)

CHAPTER 4

DISCUSSION OF RESULTS

4.1 EXTREME VALUE DISTRIBUTIONS

A theoretical explanation of the extreme value distributions was explained in Chapter 2.

4.1.1 The Effect of the Hill on the Extreme Value Distribution

As shown in Fig.4.1, the difference between the mode of the distribution U and the mean of the extreme values distribution μ is comparatively small. The only exception is at the foot of the lee side of the hill due to the strong influence by the turbulence intensity to be discussed later. The extreme value distribution also agrees with the Fisher-Tippett (Type 1) distribution which confirms that the behaviour of the extreme values over hilly terrain could be predicated confidently with adequate meteorological data.

4.2 GUST VELOCITY

The peak gust velocities recorded during the model tests have been presented as gust factors in Chapter 3 (Fig.3.14 and Fig.3.15). With this data we have an opportunity to discuss the empirical relationships predicting the gust velocity and the gust factor.

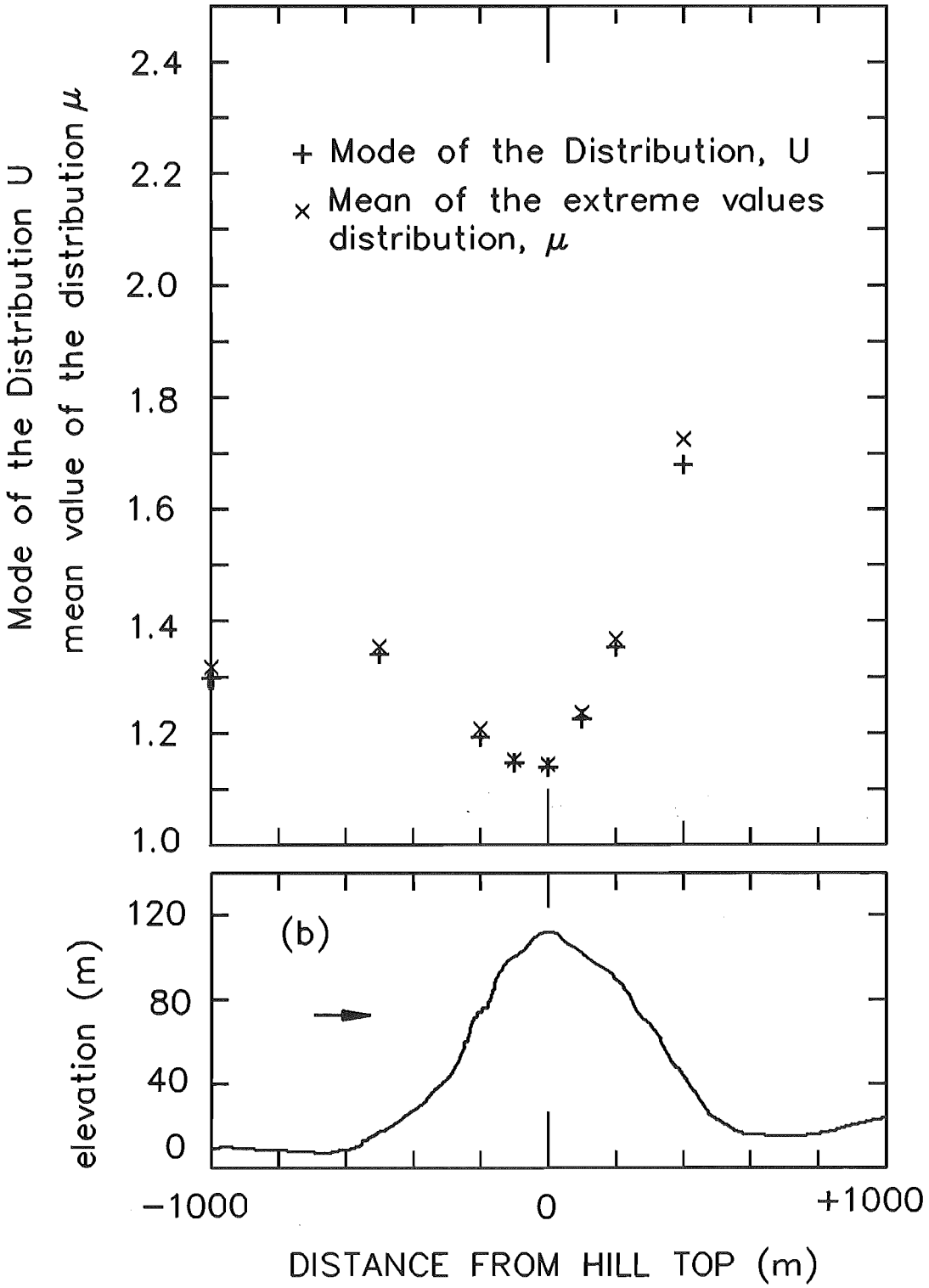

Fig. 4.1 Distribution of the Extreme Values.

According to the various empirical relationships which are discussed in Chapter 2 for the gust factors, the gust factor depends predominantly on the averaging time T_{av}, the record length T_0 and the turbulence intensity $\sigma_v/\overline{V}$ and many of the predictions except for Greenway have a common form as equations 2.31,

$$G=\hat{V}/\overline{V}=1+A\log(T_0/T_{av})$$

Where,

$$A=a(\sigma_v/\overline{V})^n$$

It was concluded by ESDU(72026) from a wide range field data that a = 2.14 and n = 1.33 (for T_{av} = 3, T_0 = 3600 seconds) but variations of these values should be expected due to the choice of T_{av} and the flow conditions.

4.2.1 Estimation of Gust Factor Constants

In order to check the empirical relationship of the gust factor between A and (a, n), A can be rewritten from equation 2.31,

$$A=\frac{(G-1)}{\log(T_0/T_{av})}$$

As explained in chapter 2.5.2, an averaging time of 3 seconds is generally used for the wind loading analysis and is commonly accepted by the engineering community for small components such as cladding.

The full scale record length T_0 for data taken in these experiments is 768 seconds. The derivation of the gust factors and turbulence intensities from the data were presented in chapter two, and thus we may obtain A for various positions over the hill.

Fig.4.2 reveals that the value of A increases on the

upwind side of the hill but just after the crest the value of A decreases suddenly to a minimum due to the rapidly increasing velocity fluctuations, after which A steadily increases.

In order to highlight the values of a,n and their variations over the hill, parameter A in gust factor equation 2.31 can be written as,

$$\log A = \log a + n\log(\sigma_v/\overline{v})$$

If the influence of the velocity fluctuations are ignored, a constant peak factor g may be assumed to exist over the hill. Then log A could be plotted on the ordinate against $\log(\sigma_v/\overline{v})$ on the abscissa in Fig.4.3 to generate a straight line according to the above equation. Therefore a and n could be obtained from this linear plot.

From this graph we find that a = 0.90 and n = 1.00.

It is quite interesting to observe that these results are similar to Bowen's results for the escarpments (1979),(a = 0.97 and n=1.0).

Then equation 2.31 could be simplified to

$$G = 1+0.9\left(\frac{\sigma_v}{\overline{v}}\right)\log\left(\frac{T_0}{T_{av}}\right) \qquad 4.1$$

Similarly, at different effective averaging times, a and n were obtained (see appendix 1). It was found that for short averaging times ($0.125 < T_{av} < 3s$), the value of a and n remained nearly constant at a = 0.9 and n = 1.0 over the hill.

The above results reveal that the value of a and n are smaller than that of ESDU (1972) where a = 2.14 and n = 1.33. The differences may be caused by the wind tunnel simulation and its significant effects on the modification of the turbulence.

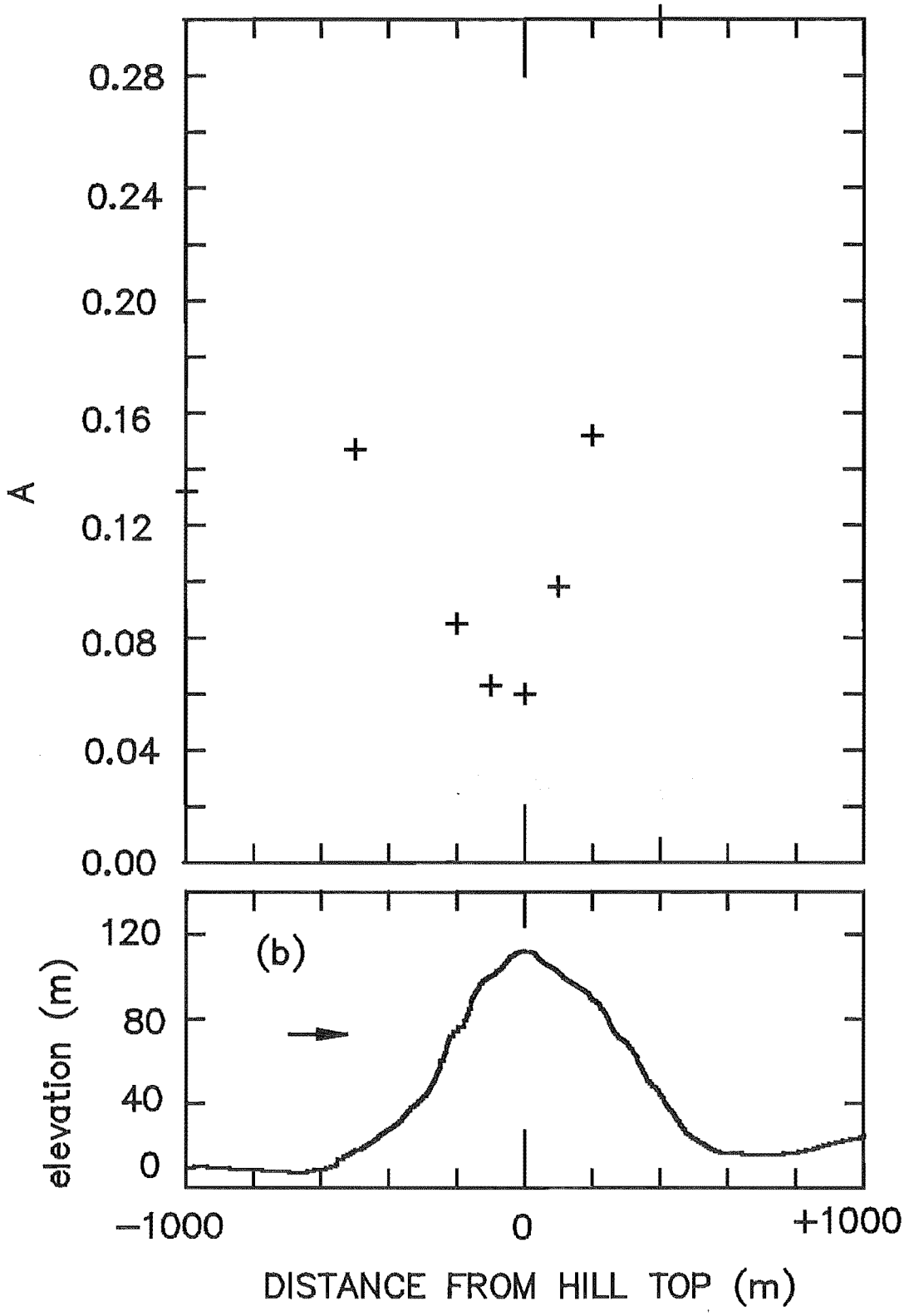

Fig. 4.2 Variation of Parameter A in Gust Factor Equation 2.31 for Flow at 10m Height. (T_{av}=3s)

It is shown in Fig.4.3. that the gust factors are directly related to the local turbulence intensity and not markedly affected by their positions on the hill except at the lee of the hill due to the flow separation. In the separated region, the flow has the character of a 3D wake with a high level of turbulence. The character of which is quite independent of the normal flow conditions outside of separated region.

Alternatively, the equation 4.1 could be simplified to,

$$G = 1+g(\sigma_v/\overline{V})$$

where g is the peak factor which depends on the choice of averaging time and record length.

This equation agrees with the empirical engineering relationship for the gust factor (equation 2.33) which is commonly used by engineers as well as the New Zealand (2/DZ 4203, 1989) and Australian (DR 87163,1987) Draft Building Codes.

Experimental and Code predictions of the gust factor by using local experiment values of turbulence intensity is shown in Fig.4.4. The sampling time gust factors are very close to the empirical relationship for the gust factors which has been adopted by the New Zealand (2/DZ 4203,1989) & (2/DZ 4203/1,1991) and Australian (DR 87163,1987) Draft Building Codes. With the averaging time increasing (3s), the value of the gust factors drop, but appears closer to the gust factors derived from equation 4.1.

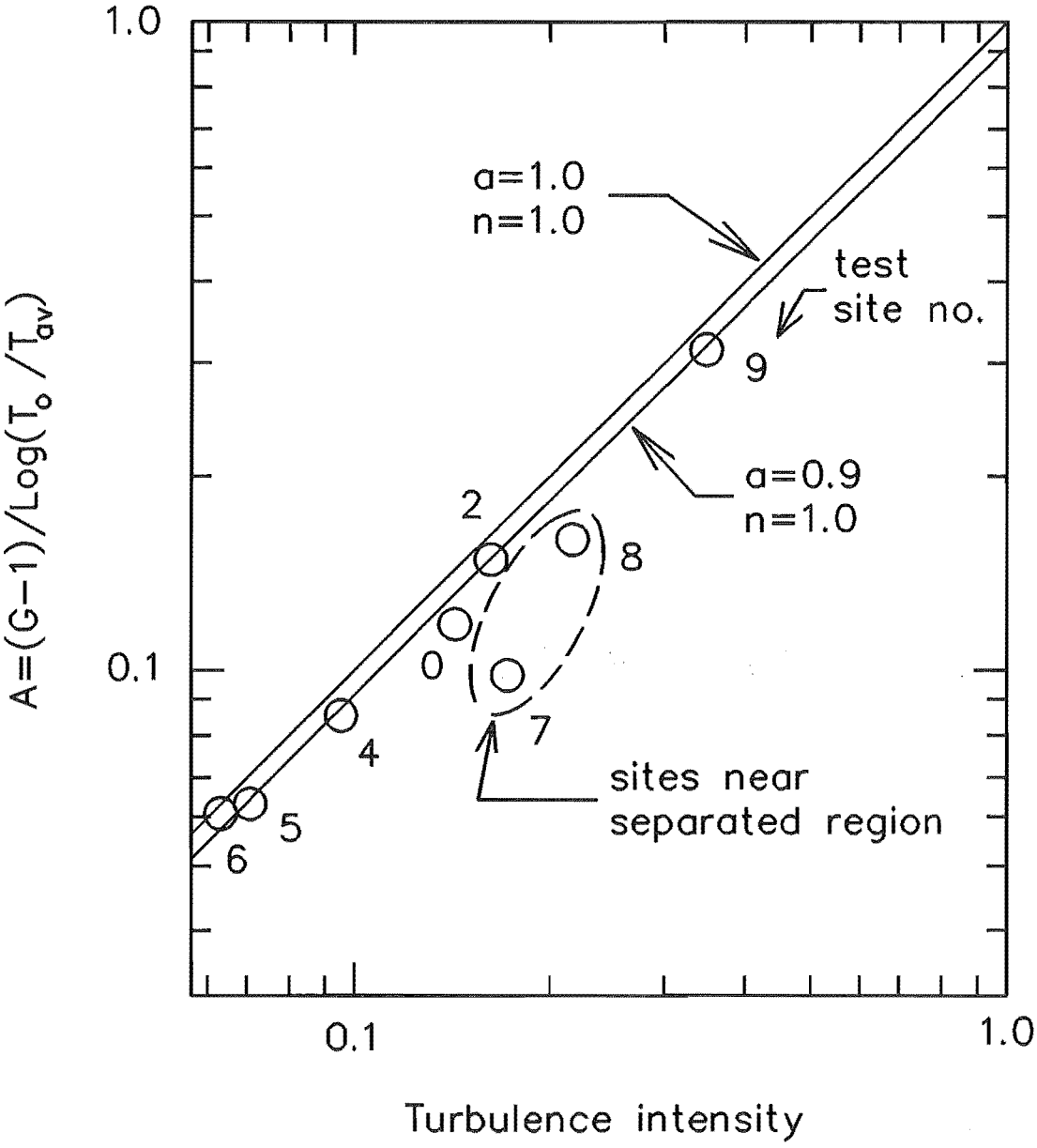

Fig. 4.3 Effect of Turbulence Intensity on the Gust Factors (T_{av}=3s), at 10m Height over the Hill.

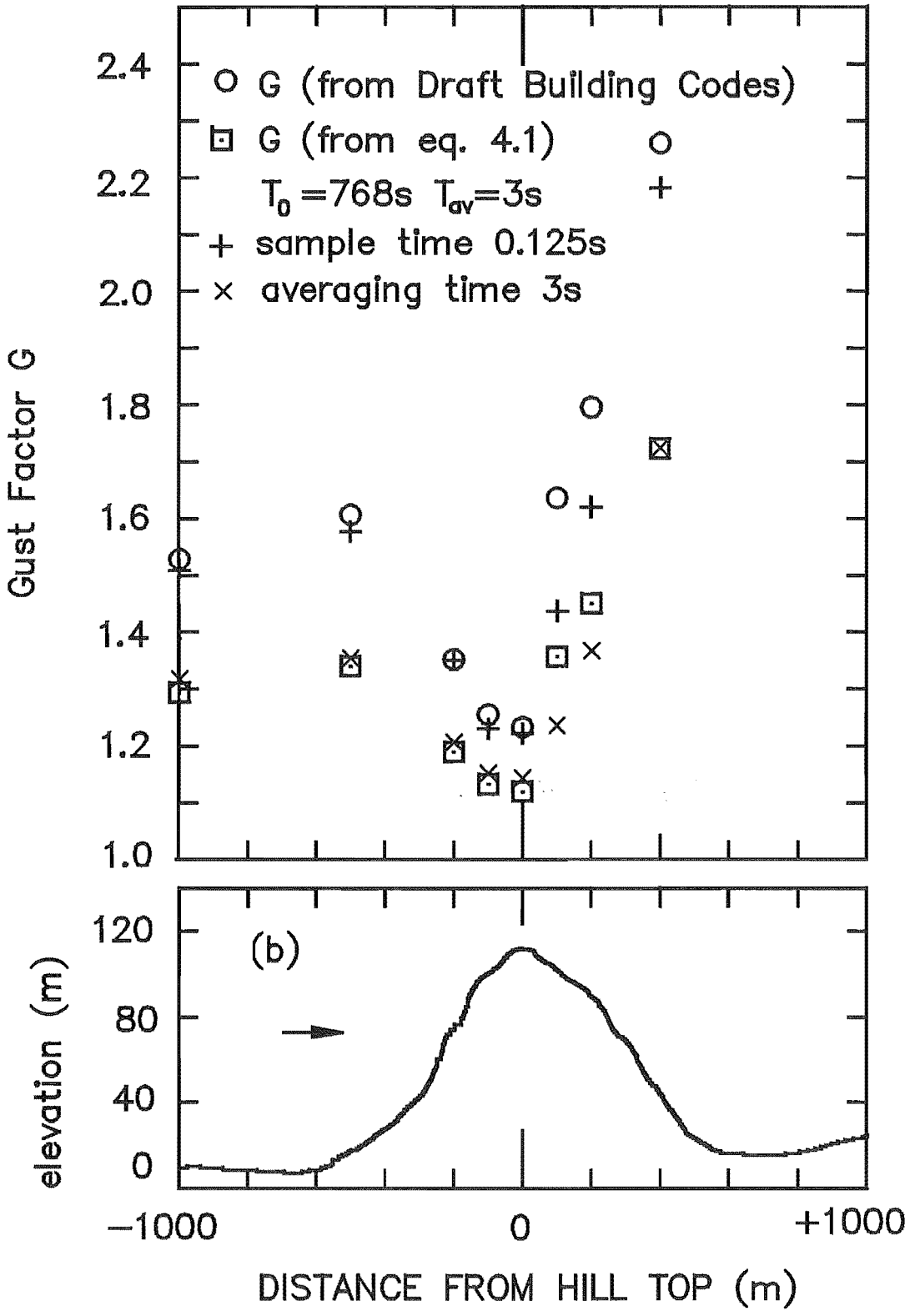

Fig. 4.4 Experimental and Code Predictions of the Gust Factor at 10m Height over the Hill.

Wieringa (1973) summarized the equation for the gust factor,

$$G = 1+\frac{\sigma}{\bar{V}}*[1.42+0.3013\ln[(T/t)-4]] \qquad 4.2$$

where :

T is record length.

t is the averaging time.

and suggested the relationship of gust factors at different record length,

$$G(t,3600) = 1.1G(t,600) \qquad 4.3$$

He also developed a model formula for the median gust factor for an arbitrary gust wavelength below 200m and for 10-min averaged wind speeds above 8m/s at a given height below 50m,

$$G(t,600) = 1+\frac{\sigma}{\bar{V}}*[1.42+0.3013\ln[(990/\bar{V}t)-4]] \qquad 4.4$$

It seems worthwhile to compare his results with equation 4.1 by using the experimental data as shown in Fig.4.5.

The gust factors obtained from both equations tend to be quite close especially on the upstream side of the hill.

4.2.2 The Effect of Averaging Time on Gust Factor

The correct selection of a suitable value T_{av} for use with the building code on hilly terrain is still under debate as discussed in chapter 2.

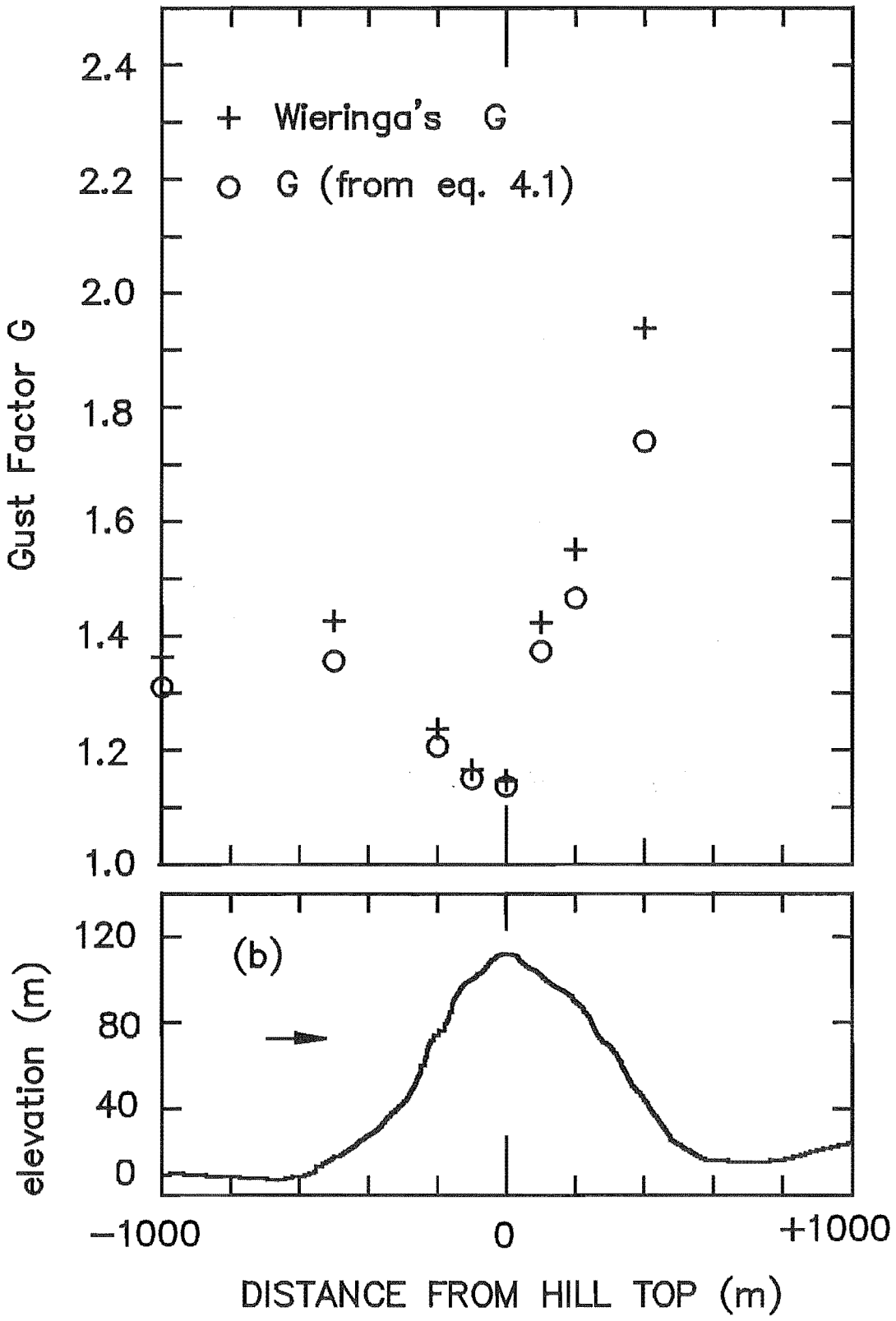

Fig. 4.5 Comparison of the Gust Factor Predictions Between Wieringa and Experimental Formula.

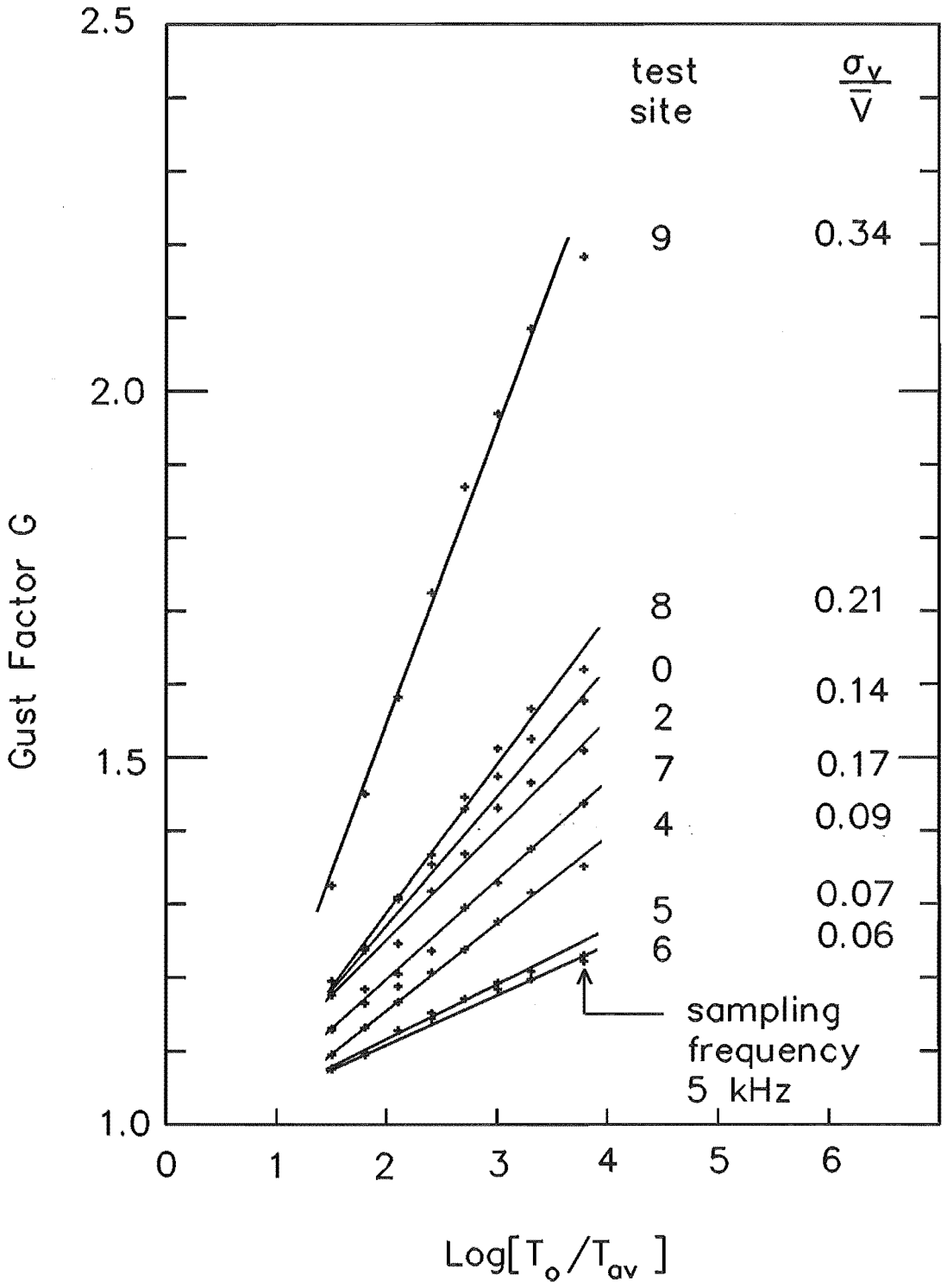

Fig. 4.6 Effect of Averaging Time on the Gust Factors Measured at 10m Height over the Hill.

It was discussed in Chapter 2 that the effective averaging time T_{av}, the record length T_0 and the turbulence intensity $\sigma/\overline{V}$ have a significant influence on the gust factor. Fig.4.6 shows the turbulence intensity at each position over the hill has been distinctly categorised and linear behaviour also proves the gust factor reliance on the effective averaging time. It could be summarized as the following equation,

$$G = 1+(\sigma_v/\overline{V})\,[\log(\frac{T_0}{T_{av}})-0.66] \qquad 4.5$$

and could be rewritten as,

$$G = 1+(\sigma_v/\overline{V})\log(\frac{T_0}{4.6T_{av}}) \qquad 4.6$$

An interesting anomaly arising here is from the commonly used empirical relationship, when the averaging time T_{av} equals the record length T_0, the gust factor should equal unity. The above equation shows the gust factor appears to be unity if the record length T_0 is 4.6 times the effective averaging time T_{av}.

An explanation for that might be found in the wind-tunnel simulation in which the air flow tends to behave more uniformly than in the field where shifts in direction and mean wind speed are prevalent. Consequently the wind-tunnel requires less time to indicate steady mean velocity and the extreme velocities would be more predictable than in a field due to a lack of fluctuations in the reference speed (assuming constant test conditions).

Although this anomaly has only a small effect on the predicted gust factor by using equation 2.31, it warrants further investigation.

4.2.3 The Estimation of a Suitable Peak Factor

Equation 2.33 is the common empirical engineering

relationship for the gust factor which has been adopted by the New Zealand (2/DZ 4203,1989) and Australian (DR 87163,1987) Draft Building Codes.

The commonly accepted value for the peak factor g is 3.7 (for T_{av} = 3 seconds, T_0 = 3600 seconds).

The peak factor basically depends on the record length T_0 and the averaging time T_{av}. The value of the predicted peak factor for this wind-tunnel experiment at 3 seconds effective averaging time is 2.17 and for the sample frequency 0.125 seconds g equals 3.8.

Comparing the above results of effective averaging time at 3 seconds, the peak factor (g = 2.17) seems smaller than that of averaging time at 3 seconds (g = 3.7) which is the commonly accepted value for the peak factor. It shows the differences between the effective averaging time in the wind-tunnel for the peak factor and the full scale averaging time equal to 3 seconds which is commonly used in the field. This anomaly requires further studies based on the consequences of the real meaning of any of the '3 second gust speed' commonly used in wind engineering (see Chapter 2).

It is interesting to note that g = 3.5 was suggested by J.D. Holmes which is different to the traditional value of 3.7. The peak factor calculated using Wieringa (1973) is 3.09. These differences are trivial when compared with the peak factor (g=2.17) obtained from this experiment.

4.2.4 The Effect of the Turbulence Intensity

If we assume the peak factor g is a constant, the gust factor is predicted to depend simply on the turbulence intensity. This dependence was confirmed by the various empirical relationships which were discussed in Chapter 2 as well as by this experiment such as in Figure 4.7.

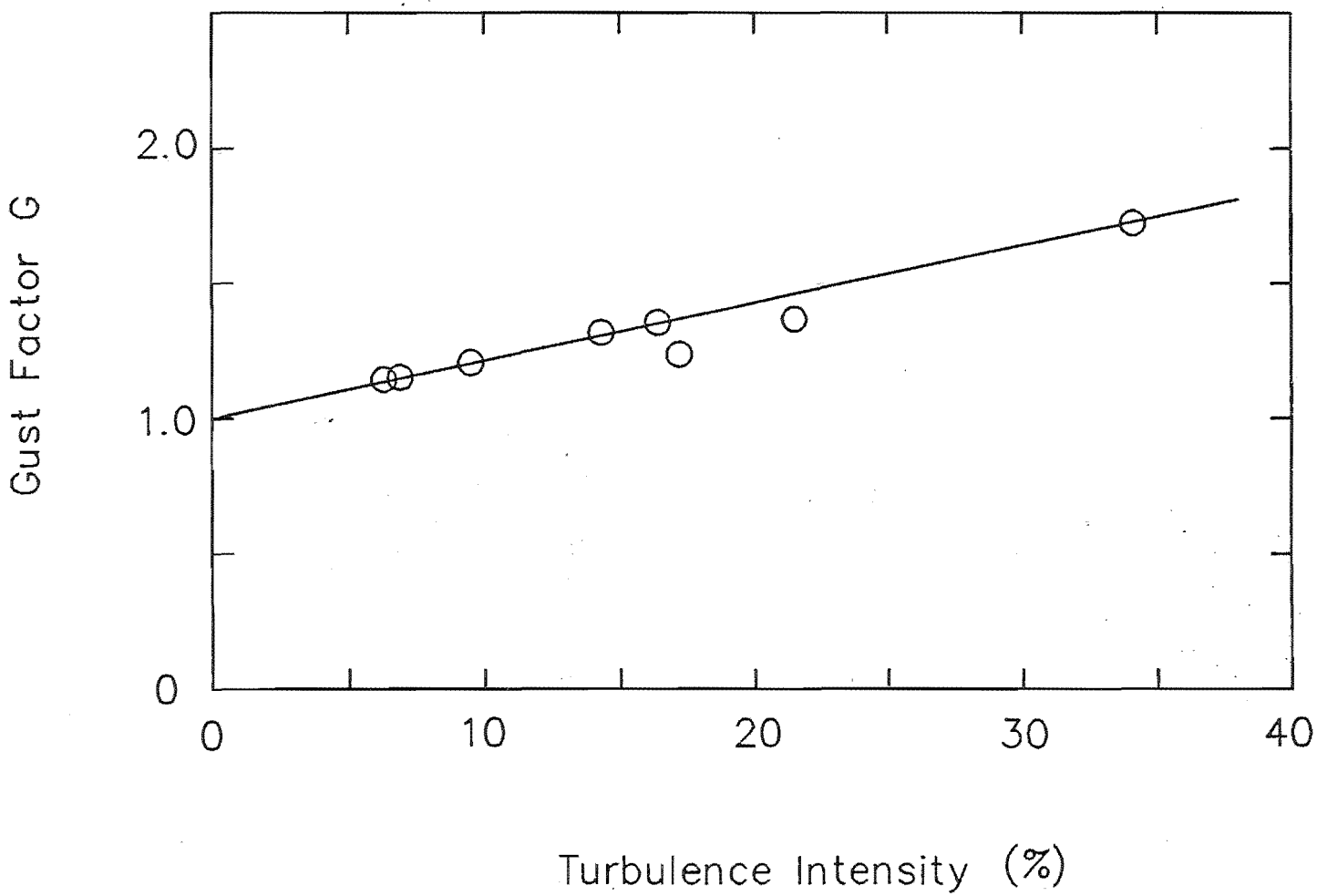

Fig. 4.7 Relationship of the Gust Factors and the Turbulence Intensities

The linear relationship between the gust factors and the turbulence intensites support the empirical engineering relationship for the gust factor (equation 2.33) which has been adopted by the New Zealand and Australian Draft Building Codes.

Regardless of the areas of flow separation in the lee of the hill, for all the other hill sites in the attached flow, the gust factor may be adequately predicted by the simple flow and data acquisition parameters contained in equation 2.31 in a similar manner to flat terrain.

4.3 MEAN GUST SPEED FRACTIONAL SPEED-UP

As it was mentioned in Chapter 2, both Codes derived their topographic multipliers ($\bar{M}_t$ and $\hat{M}_t$) from the fractional mean wind speed-up estimates derived from Taylor and Lee (1984) based on the analytical theory. The fractional mean wind speed-up is defined as equation 2.14,

$$\Delta S = (\bar{V}_h - \bar{V}_0) / \bar{V}_0$$

Where,

ΔS is the mean wind speed-up.

$\bar{V}_h$ is the local mean wind speed over the hill.

$\bar{V}_0$ is the mean wind speed at the same height upstream of the hill over open flat terrain at reference position.

Similarly, we can define the fractional mean gust speed-up ΔG as the fractional change in gust speed for further study of the behaviour of the peak gust and its influence on the Building Codes.

$$\Delta G = (\hat{V}_h - \hat{V}_0) / \hat{V}_0 \qquad 4.6$$

Where,

ΔG is the fractional mean gust speed-up.

$\hat{V}_h$ is the local mean gust speed over the hill.

$\hat{V}_0$ is the mean peak gust speed at the same height upstream of the hill over open flat terrain at reference position.

The variation of the mean gust speed-up and mean wind speed-up over the hill (for T_{av}=3 seconds) is shown in Fig.4.8. It reveals that the mean gust speed-up and mean wind speed-up behave in a similar manner over the hill. However, it appears the mean gust speed-up is lower than the mean wind speed-up. This would be due to the terrain affecting mostly the mean wind speed rather than the turbulence as noted earlier.

By the introduction of the fractional mean gust speed-up ΔG, the influence to the gust speed by the complex terrain could be clearly presented. The fractional mean gust speed-up over the hill may be predicted in a similar way to the mean wind speed-up suggested by Jackson and Hunt (1975) in equation 2.12.

4.4 WIND SPEED TOPOGRAPHIC MULTIPLIERS

Both New Zealand and Australian Building Codes attempt to predict gust speeds over hilly terrain by using a topographic multiplier M_t which is based on two assumptions addressed in Chapter 2. Further research is required on these assumptions.

4.4.1 The Effect of the Hill on the Turbulence

In chapter two, both codes derive topographic multiplier ($\overline{M}_t$ and $\hat{M}_t$) based on the assumptions that the peak gust factor is simply related to the turbulence intensity in the same manner over both flat and complex terrain, and the turbulence was convected over the hill without any change in the value of the RMS velocity.

$$(\sigma_v)_h = (\sigma_v)_0 = \sigma_v$$

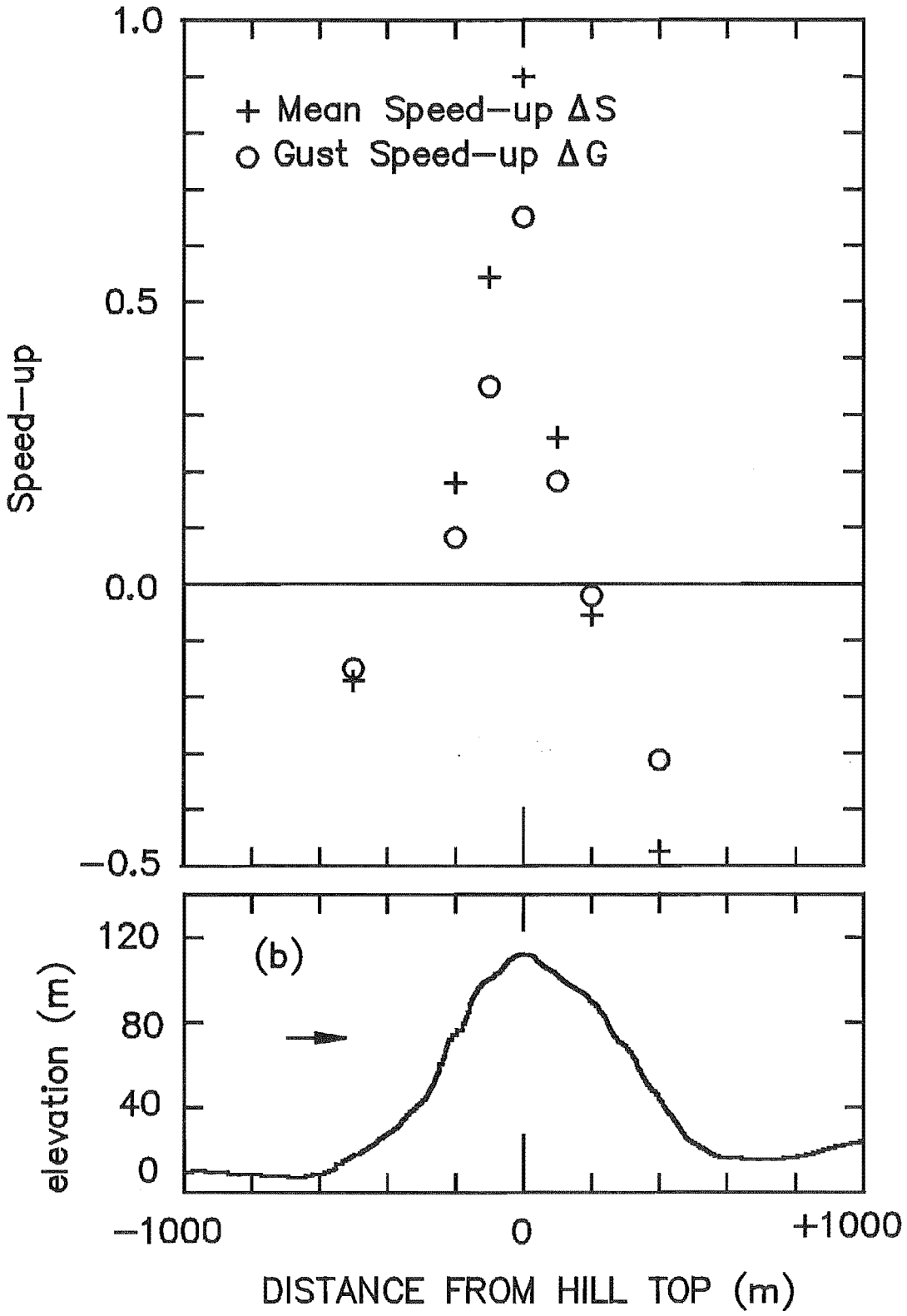

Fig. 4.8 Comparison of the Mean Gust Speed-up and Mean Wind Speed-up.

In fact in the hilly terrain, the turbulence (RMS value) depends predominantly on the shape of the hill and the position on the hill as shown in Fig.3.13. The velocity fluctuations were decreased as flow moves toward the ridge top. In the region after the crest the velocity fluctuations increased abruptly as a wake region was developed.

Counihan (1973) predicted for the three sinusoidal hill shapes that flow separation would occur when H/L > 0.43 (for H/δ = 0.125) and H/L > 0.54 (for H/δ = 0.083)

It was suggested by Taylor and Gent (1974) that the flow separation would occur over their hill shapes when H/L was greater than 0.66. Askervein Hill develops its flow separation when H/L is 0.59. This discrepency of H/L requires further investigation of the turbulence characteristics over the hill.

4.4.2 Mean Wind Topographic Multiplier

The values for the mean wind topographic multiplier Mt from the Codes have satisfactory agreement with the value obtained from the model tests as shown in Fig.4.9 except in the lee of the hill due to the separated flow which was not reproduced by the model hill. It should be noticed that the Code rules were originally derived from sources that contained the Askervein Hill data so that agreement for mean topographic multiplier $\overline{M}_t$ values should be expected.

4.4.3 Mean Gust Speed Topographic Multiplier

In order to check the empirical equation 2.41 which was adopted by both Codes, namely

$$\hat{M}_t = \hat{v}_h/\hat{v}_0 = 1+\Delta S/G_0$$

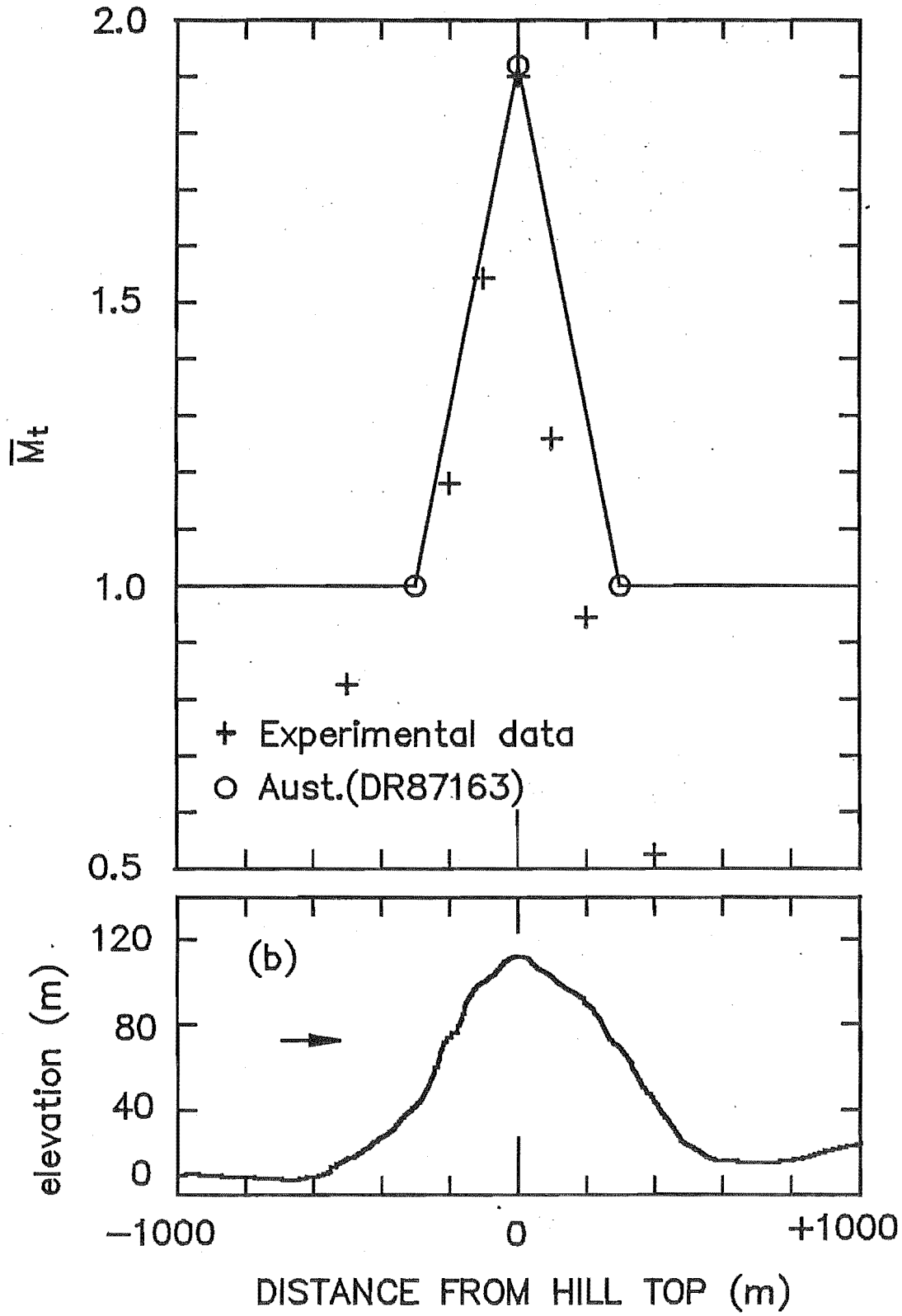

Fig. 4.9 Experimental and Code Predictions of the Mean Gust Speed Topographic Multiplier

It could be compared with the gust speed topographic multiplier equation 2.44 which was derived from the theory;

$$\hat{M}_t = \hat{V}_h/\hat{V}_0 = \Delta G - 1 = G_h/G_0 \cdot (1+\Delta S)$$

Fig.4.10 shows the experimental and Code predictions of the mean gust speed topographic multiplier ($\hat{M}_t$). The New Zealand Draft Building Code appears lower as flow moves toward the ridge. However, it is promising to see that there are some similarities between the Codes and the experimental data.

Also from equation 2.44 we can see the gust speed topographic multiplier is dependent on the ratio G_h/G_0 and the mean wind speed-up. At the same time, normalising by G_0 considerably reduces the influence which is produced by different averaging times on the gust speed topographic multiplier as shown in Fig.4.11.

4.4.4 The Relationship between the Gust Speed and Mean Wind Topographic Multipliers

The mean gust speed topographic multipliers are notably lower than the mean speed topographic multipliers from the experimental data, as shown in Fig.4.12, except at the foot of the hill. As expected this is due to the complex terrain affecting mainly the mean wind speed and the relationship of gust factors (namely the ratio G_h/G_0).

The relationship between the mean gust speed topographic multiplier $\hat{M}_t$ and the mean wind speed topographic multiplier $\bar{M}_t$ can be expressed by the following equation;

$$\hat{M}_t = \frac{G_h}{G_0}\bar{M}_t \qquad 4.7$$

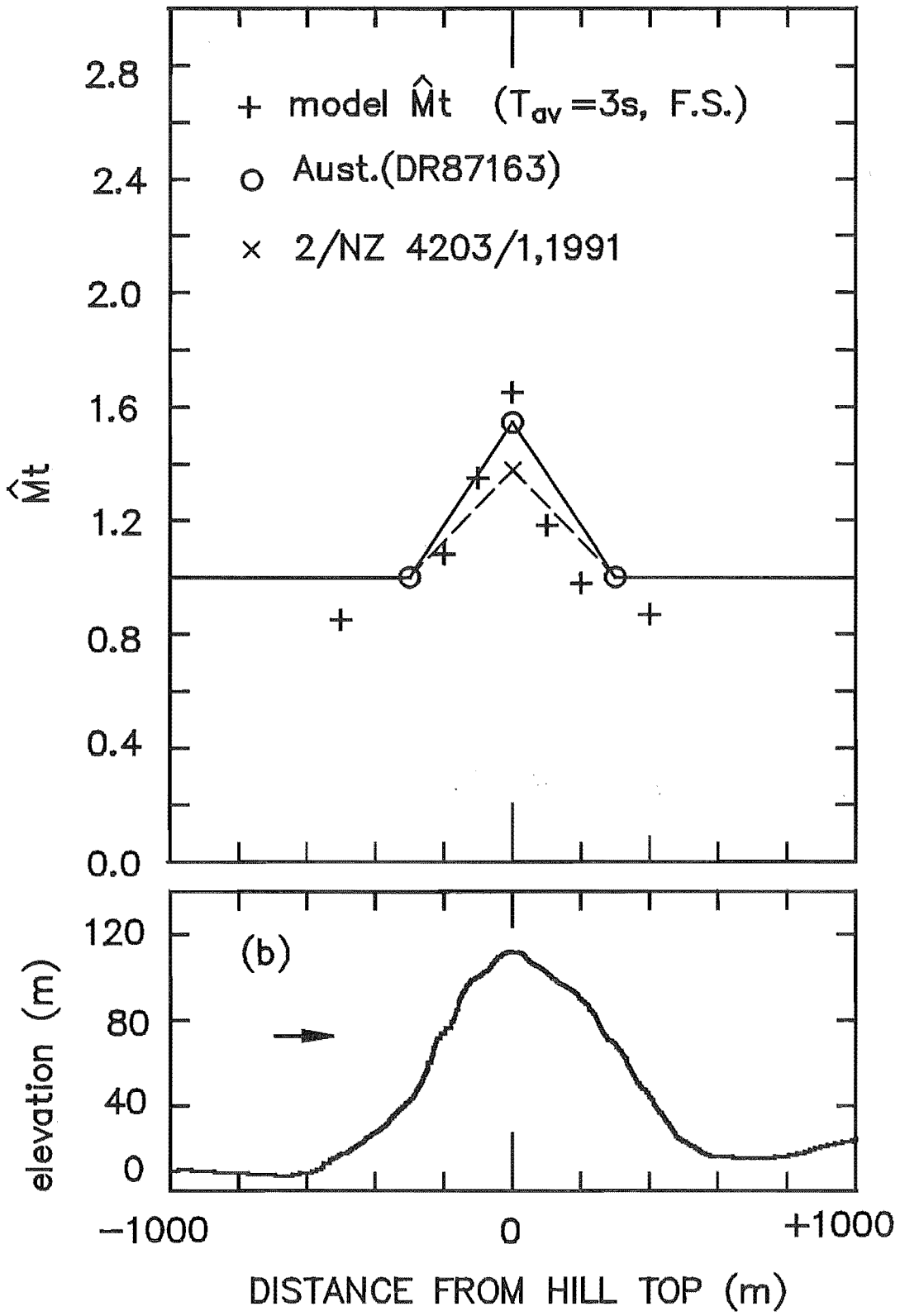

Fig. 4.10 Experimental and Code Predictions of the Mean Gust Speed Topographic Multiplier.

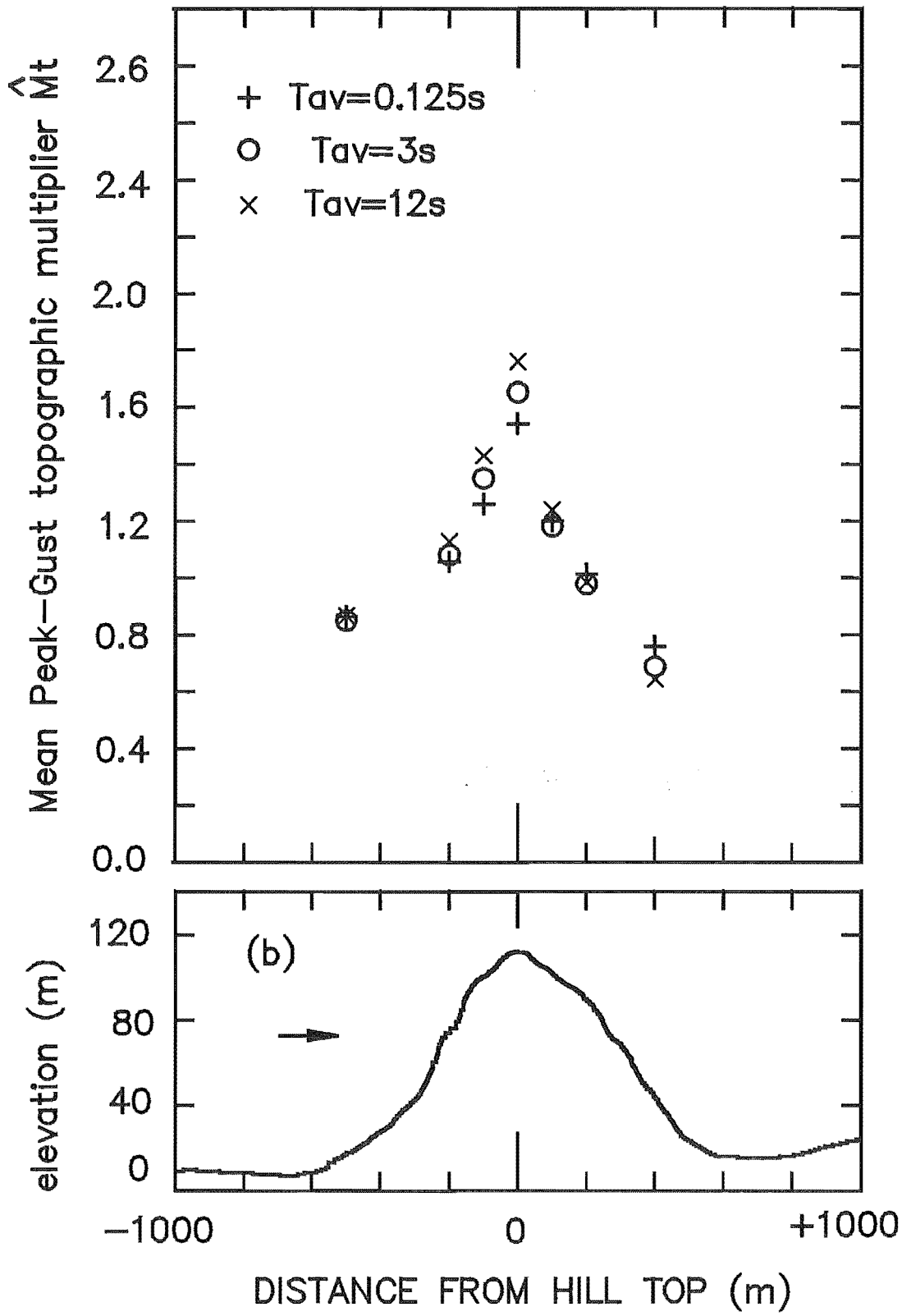

Fig. 4.11 Effect of the Averaging Time on the Mean Gust Speed Topographic Multiplier.

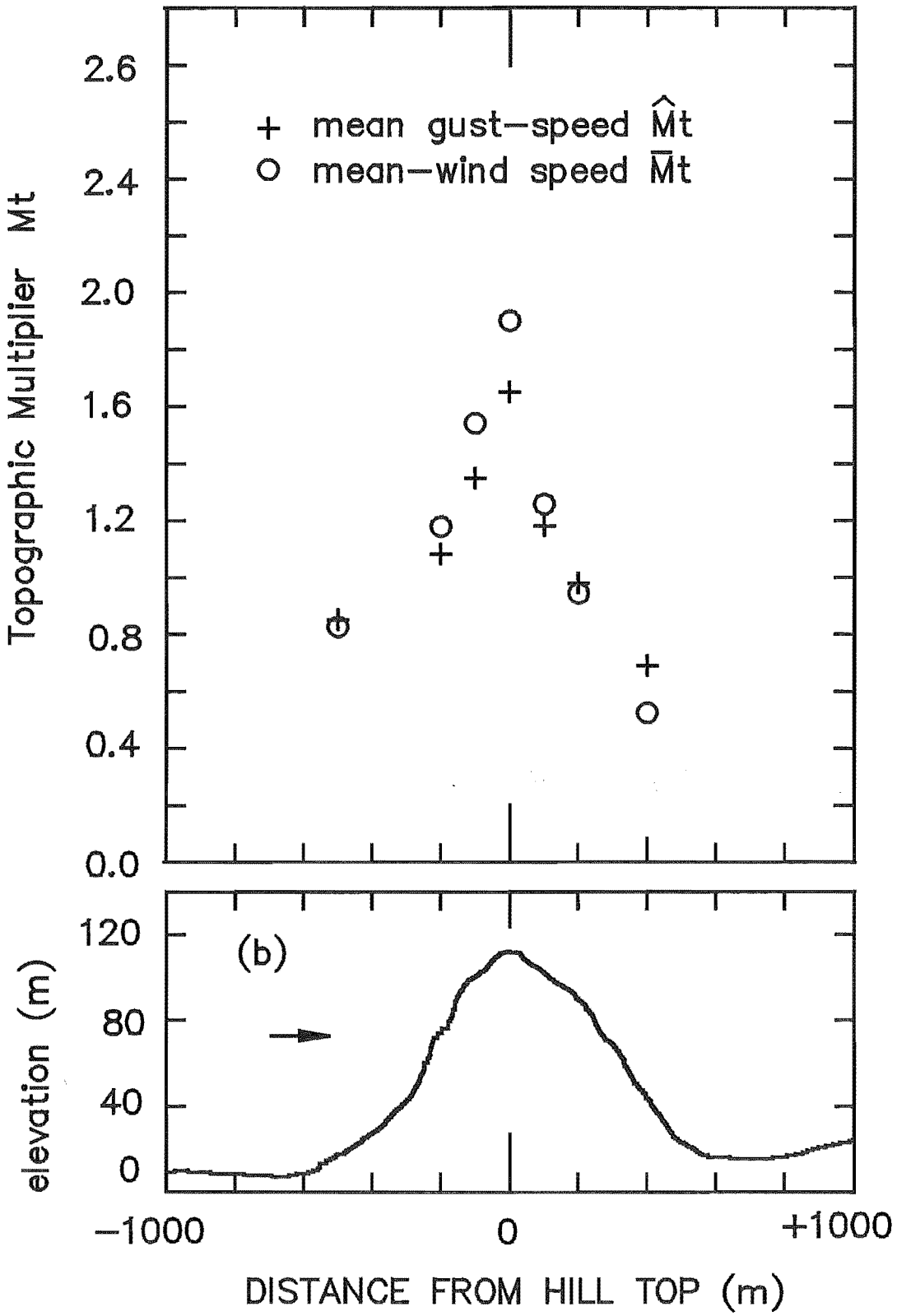

Fig. 4.12 Comparison of Mean Wind and Mean Gust Speed Topographic Multipliers from Experimental Data.

The topographic multipliers procured from the Codes were determined by using the following data from the Askervein Hill;

<1> Hill height H is 116m.
<2> Characteristic length L_u=L_d is 200m.
<3> Effective hill slope Φ (= $H/2L_u$) is 0.29 along line A, so Φ is equal to 0.26 for the 210° wind direction.
<4> Surface roughness category 2 (Roughness length z_0 is 0.03m).

As the Code rules were originally derived from sources close to the Askervein Hill data, good agreement for mean wind topographic multiplier $\bar{M}_t$ values between the Codes and the experimental data was expected.

The good agreement between the gust-speed topographic multipliers indicated by the Code rules for complex terrain and those derived from the experimental data supports the assumptions used in their derivation within the tolerance of the differences.

The new edition of New Zealand Draft Building Code (2/DZ 4203/1,1991) specifies the topographic multiplier, M_t, shall be taken as the maximum of the profile multiplier, M_p, the lee multiplier, M_l, and the channelling multiplier, M_c. The profile multiplier M_p was considered as the topographic multiplier $\hat{M}_t$ in NZ.(2/DZ 4203,89) as well as in this project.

The topographic multiplier M_t which is clarified in the New Zealand Draft Building Code (2/DZ 4203/1,1991) has simplified the design work for engineers but may cause some inaccuracy of wind loading (as shown in Fig.4.10) and warrants further studies.

4.5 CONCLUSIONS

The distribution of the extreme values of the gust factor largely depended on the shape of the hill but the dispersion of the extreme values is quite small. This extreme value

distribution agrees with the Fisher - Tippett distribution which faithfully represents the behaviour of extreme winds in the well behaved wind climates of temperate latitudes, and could be predicted confidently with adequate meteorological data.

The gust factors over the simple hill obtained from the model tests appear directly related to the local turbulence intensity, averaging time and record length which agree with the empirical relationship for the gust factor adopted by the New Zealand and Australian Draft Building Codes, namely, equation 2.31. However, the gust factors are also largely independent of special hill effects. Therefore, for the attached flow it could be adequately predicted by the simple flow and data acquisition parameters contained in equation 2.31 based on flat terrain. For given T_0, T_{av}, gust factor G is dependent solely on turbulence intensity.

A peak factor of 2.17 at 3s effective averaging time was obtained from experimental data which is smaller than the commonly accepted value of 3.7 and requires further study.

The turbulence (RMS value) changes with the various positions above the complex terrain. Particularly in those regions, such as after the crest of the hill, the turbulence increased abruptly as a wake region is developed.

Mean gust speed topographic multiplier which was adopted by the New Zealand and Australian Draft Building Codes can be related to the gust factors reported in equation 2.45. This shows that the topographic multiplier is dependent on the ratio G_h/G_0. Normalising by G_0 considerably reduces the overall effect from the choice of the averaging time and the accuracy of the gust speed topographic multiplier $\hat{M}_t$ can be improved.

CHAPTER 5

CONCLUSIONS

The objectives of this project have been mentioned in Chapter One and the conclusions at each stage have been given at the end of each Chapter. However, it is informative to summarise the main conclusions of the experimental work presented in this project and recommend future work.

5.1 SUMMARY OF CONCLUSIONS

1) The background theory discussed in Chapter Two showed the need of supporting experimental work concerned with investigating of the behaviour of the extreme values over the complex terrain.

2) Experimental work in the wind-tunnel showed the similarity of the gust factors to that predicted by empirical relationships. The data acquisition system was adequate enough for the measurement of the wind characteristics.

3) The distribution of the extreme gust factor values largely depended on the shape of the hill but the dispersion of the extreme values is fairly small. However in the lee of the hill dispersion was largely due to the strong turbulence intensity in the wake region.

4) Gust factors over the simple hill are directly related to the local turbulence intensity and largely independent of special hill effects. Therefore, it could be adequately predicted by the simple flow and data acquisition parameters contained in equation 2.31.

5) Mean gust speed topographic multiplier which was adopted by the New Zealand and Australian Draft Building Codes could be related to the gust factors reported in equation 2.44. It shows that the topographic multiplier is dependent on the ratio G_h/G_0. Normalising by G_0 considerably reduces the overall effect from the choice of the averaging time.

6) Comparing the values adopted by the New Zealand and Australian Draft Building Codes for peak gust speeds over a simple hill with recent wind-tunnel model test, regardless of the common origins of the topographic multiplier in the Codes rules, some differences occurred between the Codes and the experimental results due to the differences in the definition of the gust speed averaging time.

However good agreement has been found between the predictions of the analysis by the Code rules for complex terrain and those derived from the experimental data. Therefore, both Codes could be used reasonable adequately for the prediction of the extreme values.

5.2 RECOMMENDATIONS FOR FURTHER RESEARCH

1) The idea of the effective gust-speed averaging time used in the wind-tunnel simulation and the commonly accepted relationship between the averaging time and the size of the structure or structural element concerned needs further clarification.

2) Model and full scale field tests in a wide range of complex terrain and different flow conditions are required for checking the Building Code rules.

3) An effective and better prediction method for the extreme value requires further research and would be a tremendous contribution to the Building Code and various applications in the wind engineering area.

REFERENCES

Baker C.J., Wood C.J. and Gawthorpe (1985). Strong Winds in Complicated Hilly Terrain-Field Measurements and Wind-Tunnel Study. Journal of Wind Engineering and Industrial Aerodynamics. 18(1985) 1-26.

Bendat J.S. and Piersol A.G. (1971). Random Data: Analysis and Measurement Procedures. Wiley.

British Standards Institute Code of Practice (1972). CP3, Ch. V, Pt.2, Wind Loads.

Bowen A.J. (1979). Some Effects of Escarpments on the Atmospheric Boundary Layer. PhD thesis, University of Canterbury.

Bowen A.J. (1981). Engineering Aspects of the Wind. Weather and Climate. Journal of the Meteorological Society of New Zealand. Vol.1, No.1, February 1981.

Bowen A.J.(1983). The Prediction of Mean Wind Speeds above Simple 2D Hill Shapes. Journal of Wind Engineering and Industrial Aerodynamics, 15(1983) 259-270.

Bowen A.J. and H.W. Teunissen (1987). The Askervein Hill Project. Research Report No. 86-7. Wind-Tunnel Simulation at Length Scale 1:2500 (Part 1). Tests at the Atmospheric Environment Service. Atmospheric Environment Service, Canada.

Bowen A.J. and Calvert B. (1987). The Askervein Hill Project. Wind Tunnel Simulation at Length Scale 1:2500 (Part 2). University of Canterbury, Mechanical Engineering Report No.38.

Bowen A.J., Zheng Hong and D.E.Stock (1989). The Variation of Peak-Gust Speeds Over an Isolated Hill. Proc. Tenth

Australasian Fluid Mechanics Conference, University of Melbourne, Australia.

Britter R.E., Hunt J.C.R. and Richards K.J.(1981). Air Flow Over a Two-Dimensional Hill: Studies of Velocity Speed-up, Roughness Effects and Turbulence. Quart. J.R. Met. Soc.(1981), 107 pp 91-110.

Counihan J.(1973). Flow Over Two-Dimensional Hills and Plateaux in Simulated Boundary Layer Flow. Central Electricity Research laboratories Note No. RD/L/N277/73, UK.

Davenport A.G. (1964). Note on the Distribution of the Largest Value of a Random Function with Application to Gust Loading. Proc. Inst. Civil Engineers, 28 pp 187-196.

Davenport A.G. (1967). The Dependence of Wind Loads on Meteorological Parameters. Proc. Second International Conference on Wind Effects on Buildings and structures. Ottawa, Canada: 19-82.

Deaves D.M. and Harris R.I. (1976). A Mathematical Model of the Structure of Strong Winds. Environmental Sciences Research Unit Report No 24. Cranfield, UK. (CIRIA Report No 76.)

DR87163 (1987). Minimum Design Load on Structures. Part 2-wind Forces. Draft Australian Standard for comment. SAA Sydney, Australia.

2/DZ 4203 (1989). General Structural Design and Design Loadings for Buildings. Part 4 Wind Load Provisions. Draft Code for comment. SANZ, New Zealand.

2/DZ 4203/1 (1991). General Structural Design and Design Loadings for Buildings. Part 4 Wind Load Provisions. New Zealand.

ESDU 72026 (1972). Characteristics of Wind Speed in the Lower Layers of the Atmosphere Near the Ground: Strong Winds (neutral atmosphere) Engineering Sciences Data Unit, London, UK.

ESDU (1974). Characteristics of the Atmospheric Turbulence near the Ground. Engineering Sciences Data Unit, London, UK.

Flay R.G.J. (1978). Structure of a Rural Atmospheric Boundary Layer near the Ground. PhD thesis. Dept. Mechanical Engineering, University of Canterbury, Christchurch, New Zealand.

Greenway M.E. (1979). An Analytical Approach to the Wind Velocity Gust Factors. Jour. Industrial Aerodynamics 5 pp61-91.

Holmes J. D.(1986). Introduction to Wind Engineering.

Hunt J.C.R. (1973). A Theory of Two-Dimensional Flow round Two-Dimensional Bluff Bodies, J. Fluid Mech.,61,625-706.

Jackson P.S. and Hunt J. C. R. (1975). Turbulent Wind Flow over a Low Hill. Quart. Journal Royal Meteorological Society, 101 pp929-955.

Mackey S. (1970). Wind Studies in Hong Kong - Some Preliminary Results. Industrial Aerodynamics Abstracts. 5: 1-16.

Mayne J.R. and Cook N.J. (1976). On Design Procedures for Wind Loading. Note No N 134/76. Building Research Establishment, Department of the Environment, Garston, UK.

Mayne J.R. (1979). The Estimation of Extreme Winds. Jour. Industrial Aerodynamics 6 pp109-137.

NZS 4203 (1976). Code of Practice for General Structural Design and Design Loadings for Buildings. Part 4 Wind Loads.

SANZ, New Zealand.

Pearse J.R. (1979). The Influence of Two-Dimensional Hills on Simulated Atmospheric Boundary Layers. PhD thesis. University of Canterbury.

Taylor P.A. and Gent P.R. (1974). A Model of Atmospheric Boundary Layer Flow above an Isolated Two-Dimensional 'Hill'; An Example of Flow above 'Gentle Topography'," Boundary-Layer Meteorology, 7, pp 349-362,1974.

Taylor P.A. and Lee R.J. (1984). Simple Guidelines for Estimation Wind Speed Variations due to Small Scale Topographic Features. Climatological Bulletin 18, no2 pp3-32.

Taylor P.A. and Teunissen H.W. (1987). The Askervein Hill Project: Overview and background data. Boundary-Layer Meteorology 39 pp15-39.

Tomlinson A.I. The Wind Programme of the New Zealand Meteorological Service. N.Z. Meteorological Service.

Townsend, A.A. (1972). Flow in a Deep Turbulent Boundary Layer over a Surface Distorted by Water Waves, Ibid.,55, 719-735.

Teunissen H.W. (1970). Characteristics of the Mean Wind and Turbulence in the Planetary Boundary Layer. Institute for Aerospace Studies, University of Toronto, UTIAS review No. 32:221 pp.

Teunissen H.W., Shokr M.E., Bowen A.J., Wood C.J. and Green D.W.R. (1987). The Askervein Hill Project. Wind Tunnel Simulations at Three Length Scales. Boundary-Layer Meteorology 40 pp1-29.

Wieringa J. (1973). Gust Factors over Open Water and Built-up Country. Boundary-Layer Meteorology, 3:424-441.

APPENDIX 1

Parameter a and n of A in Gust Factor Equation 4.1.

Averaging time T_{av} (s)	a	n
0.125	0.94	1.0
0.375	0.945	1.0
0.75	0.945	1.0
1.5	0.94	1.0
3.0	0.90	1.0
6.0	0.86	1.0
12.0	0.74	1.0
24.0	0.60	1.0

APPENDIX 2(a)

DRAFT NEW ZEALAND STANDARD
Taken from 2/DZ 4203/1 (CPT KMcI 37) 16.01.91

GENERAL STRUCTURAL DESIGN AND DESIGN LOADINGS FOR BUILDINGS
PART 4
WIND LOAD PROVISIONS

STANDARDS ASSOCIATION OF NEW ZEALAND
Private Bag, Wellington

4.4.5
Shielding multiplier, M_s

4.4.5.1
The shielding multipliers, M_s, shall be taken from table 4.4.4. Where the effects of shielding are ignored or are not appropriate for a particular wind direction, M_s shall equal 1.0 for that direction.

4.4.5.2
The shielding parameter, s, in table 4.4.4 shall be determined from:

$$s = \frac{l_s}{\sqrt{(h_s b_s)}} \quad \ldots\ldots\ldots \text{(Eq. 4.4.2)}$$

$$\text{where } l_s = h_t \left(\frac{10}{n_s} - 5 \right) \ldots\ldots\ldots\ldots\ldots\ldots \text{(Eq. 4.4.3)}$$

4.4.5.3
For the purposes of 4.4.5 shielding buildings are those within a 45° sector of radius 20 h_t (symmetrically positioned about the directions being considered) and whose height is greater than or equal to z.

TABLE 4.4.4
SHIELDING MULTIPLIER, M_s

Building spacing parameter (s)	Shielding multiplier (M_s)
< 1.5	0.7
3.0	0.8
6.0	0.9
>12.0	1.0

NOTE - For intermediate values of s, interpolation is permitted.

4.4.6
Topographic multiplier, M_t

4.4.6.1
The topographic multiplier, M_t, shall be taken as the maximum of the profile multiplier, M_p, the lee multiplier, M_L, and the channelling multiplier, M_c.

4.4.6.2
Profile multiplier, M_p
The (landform) profile multiplier, M_p, shall equal 1.0 except where the site is within a local topographic zone as defined in figs. 4.4.2

(a) and (b). In such cases the profile multiplier applicable to the site shall be obtained by interpolating the crest value, established from Table 4.4.5, and the value at the boundary, where M_p=1.0. The interpolation shall be based on the horizontal distance from the crest and on the height above ground (z).

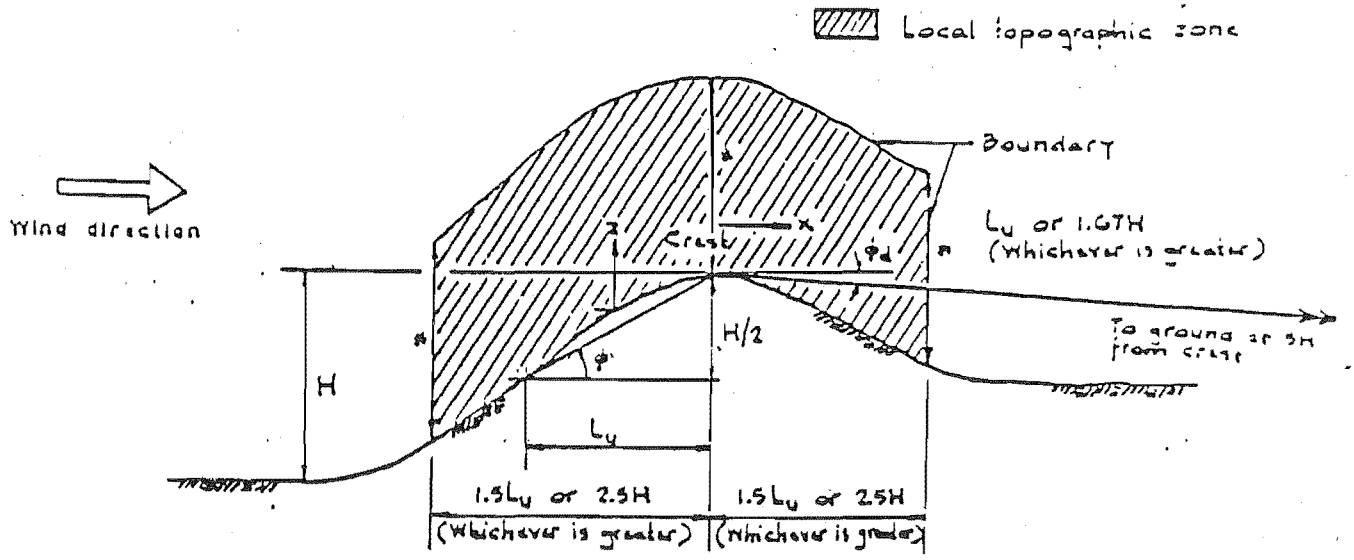

Fig. 4.4.2(a)
DEFINITION OF THE LOCAL TOPOGRAPHICAL ZONE - HILLS AND RIDGES

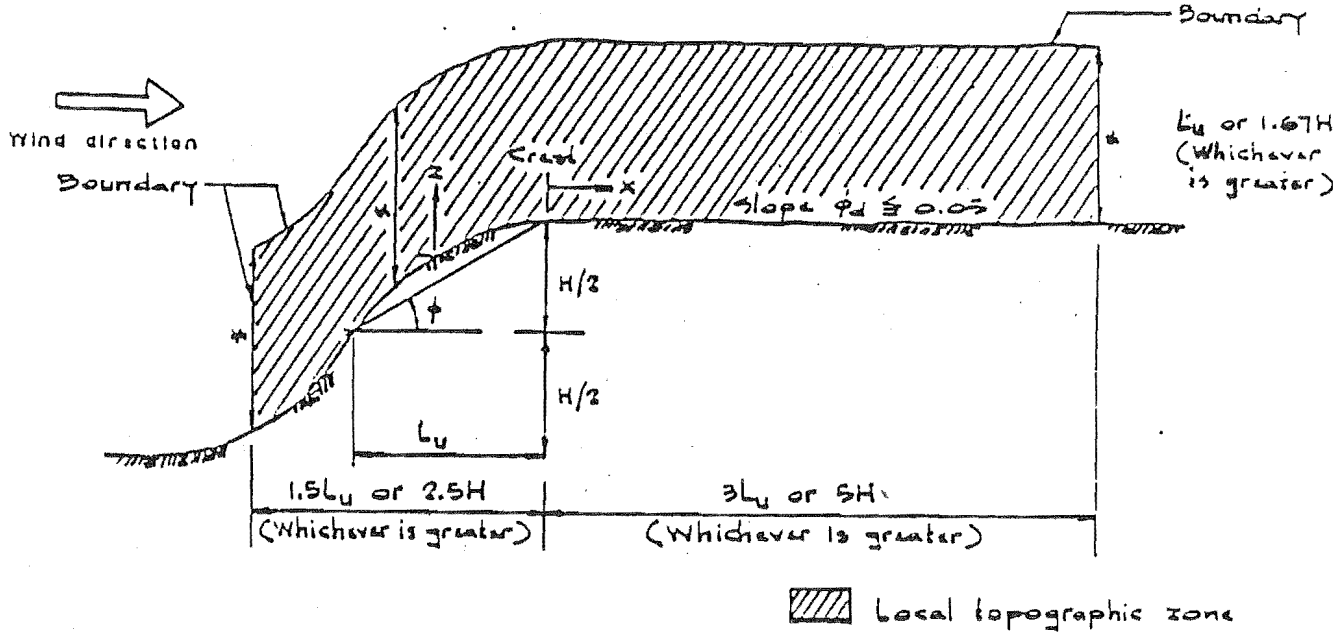

Fig. 4.4.2 (b)
DEFINITION OF THE LOCAL TOPOGRAPHICAL ZONE - TWO-DIMENSIONAL ESCARPMENTS

TABLE 4.4.5
PROFILE MULTIPLIER, M_p AT CREST (z = o)

Up-wind slope (ϕ)	Land profile multiplier, M_p	
	Escarpments $\phi_d \leq 0.05$	Hills and ridges, $\phi_d \geq 0.10$
0.05	1.04	1.09
0.1	1.08	1.18
0.2	1.16	1.36
$\geq$ 0.3	1.24	1.54

NOTES - For intermediate values of either up-wind slope (ϕ), or down-wind slope (ϕ_d), linear interpolation is permitted.

4.4.6.3
Lee multiplier, M_L
The lee (effect) multiplier, shall equal 1.0 unless the site is within one of the lee zones as indicated in figs. 4.4.1(a) or (b). Each lee zone is considered to be 30 km in width, measured from the leeward crest of the initiating range, in the direction of the wind nominated as being effected in the particular zone. The lee zone comprises a "shadow lee zone", which extends 12 km from the upwind boundary of the lee zone, and an "outer lee zone" over the remaining 18 km.

The lee multiplier equals 1.35 for sites within the shadow lee zone, and, within the outer lee zone, the lee multiplier shall be determined by linear interpolation with horizontal distance from the shadow/outer zone boundary (where M_L=1.35), and the downwind lee zone boundary (where M_L=1.0).

The lee multiplier shall apply only to wind from the direction nominated.

4.4.6.4
Channelling multiplier, M_c
The channelling multiplier shall equal 1.0 except where local hill formations initiate a funnelling effect, where it shall, depending on the characteristics of the valley, have a value of between 1.0 and 1.25 which is applied to wind in the up-valley direction.

4.4.7
Structure importance multiplier, M_i

4.4.7.1
The structure importance multiplier M_i, shall be as given in table 4.4.6.

TABLE 4.4.6
STRUCTURE IMPORTANCE MULTIPLIER, M_i

Class of structure	Multiplier, M_i
Category I	1.1
Categories II, III and IV	1.0
Category V	0.9

4.5
DESIGN WIND PRESSURE

4.5.1
The design wind pressure, q_z, at a height, z, shall be calculated from:

APPENDIX 2(B)

DRAFT FOR COMMENT

STANDARDS ASSOCIATION OF AUSTRALIA
Committee DB/6--LOADING ON STRUCTURES

DRAFT
AUSTRALIAN STANDARD
MINIMUM DESIGN LOADS ON STRUCTURES
PART 2--WIND FORCES
(REVISION OF AS 1170, PART 2--1983)

3.1.7 Local topographical effects. The wind speed at a site shall be corrected for topography if the average slope in the surrounding terrain exceeds 0.05 in any direction. The wind speed at the local height, z, shall be obtained by multiplying the wind speed above flat, level terrain at the same height z by a factor for topographical effects, M_t. 97

M_t shall be obtained by one of the following three methods:

(a) From full-scale measurements at the site.

(b) From correctly-scaled wind tunnel tests.

(c) For simple escarpments, ridges or axisymmetric hills, M_t can be obtained from Table 3.1.7 for structures where the height ratio z/L_e is less than 0.05. For structures outside this limit, see Commentary below Figure 3.1.7.

TABLE 3.1.7

TOPOGRAPHIC MULTIPLIERS AT CREST (x = 0)

Effective slope (Φ_e)	Gust velocity multiplier (M_t)		
	Escarpments	Axisymmetric hills	Ridges
0.05	1.04	1.08	1.10
0.1	1.08	1.17	1.21
0.2	1.17	1.34	1.42
≥0.3	1.25	1.50	1.63
	Mean velocity multiplier, $\bar{M}_t$		
0.05	1.07	1.14	1.18
0.1	1.14	1.28	1.35
0.2	1.28	1.56	1.71
≥0.3	1.42	1.85	2.06

NOTES:

1. Multipliers are presented for z = 10 m, Terrain Category 2.

2. The effective slope of the hill, Φ_e is given by $h/2L_e$ where L_e is the effective length of the hill as defined in Figure 3.1.7, and h is the height of the hill.

3. For intermediate values of Φ_e, use linear interpolation.

4. An escarpment has a value of $h/2L_d$ of 0.05 or less. A ridge or axisymmetric hill has a value of $h/2L_d$ greater than 0.05.

5. For locations upwind or downwind of the crest, linear interpolation with x should be carried out from the value given in Table 3.1.7 to a value of 1.00 at $x = -1.5L_e$ and $+1.5L_d$, for hills and ridges, or $+3L_e$, for escarpments.

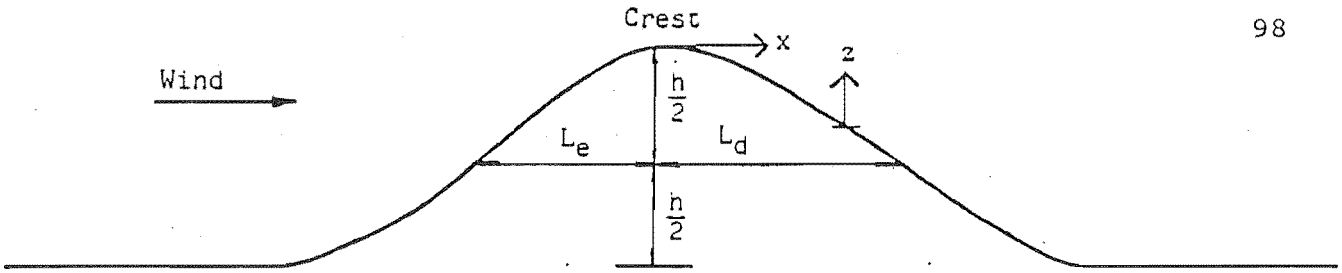

FIGURE 3.1.7. SIMPLIFIED TOPOGRAPHY

Commentary.

The wind speed at any given site is influenced by local topographical features such as funnelling or expansion in valleys, hills and escarpments. Where there is doubt, local meteorological advice shall be sought or recourse to model studies must be made to determine appropriate design wind speeds in the presence of significant local topographical features. The most critical conditions occur near the top of a steep rise, cliff, bluff or escarpment and rules for these situations are given. The rules follow the guidelines given by Taylor and Lee (Ref. 10) and Bowen (Ref. 11), which are based on extensive full scale and wind tunnel studies and theoretical work by Jackson and Hunt (Ref. 12).

For height ratios z/L_e greater than 0.05 but less than 1.0, the topographic multipliers are less than those given in Table 3.1.7. General equations for the multipliers M_t and $\bar{M}_t$ are as follows:

$$M_t = 1 + \frac{K_t s \Phi_e}{[1 + 3.7(\sigma_v/\bar{V}_z)]} \qquad \text{for gust speeds,}$$

$$\bar{M}_t = 1 + K_t s \Phi_e \qquad \text{for mean speeds}$$

where

$$s = \left(1 - \frac{|x|}{1.5L^*}\right)\exp^{-(2.5z/L_e)} \qquad \text{for } \Phi_e \leq 0.3$$

$$s = \left(1 - \frac{|x|}{1.5L^*}\right)\exp^{-(1.5z/h)} \qquad \text{for } \Phi_e \leq 0.3 \text{ (steep slopes)}$$

for negative values of x : $L^* = L_e$

for positive values of x : $L^* = L_d$ (hills and ridges)
$L^* = 2L_e$ (escarpments)

K_t = 1.6 for two-dimensional escarpments

4.0 for two-dimensional ridges

3.2 for axi-symmetric hills

Φ_e = effective upwind slope of an escarpment, ridge or hill, maximum value is 0.30.

$\sigma_v/\bar{V}_z$ = turbulence intensity in the approach flow at height z.

x = horizontal coordinate with origin at the crest

z = height above local ground level.

99

For values of z/L_e greater than 1.0, topographic effects are negligible and can be ignored.

Example calculation:

Axisymmetric Hill ($K_t = 1.6$)

Terrain Category 3

z = 20 m
h = 150 m
L_e = 750 m
x = −200 m (site on upwind slope)

$$\Phi_e = \frac{h}{2 \times L_e} = \frac{150}{2 \times 750} = 0.10$$

$$s = [1 - \frac{|x|}{1.5L_e}] \, e^{-(2.5z/L_e)}$$

$$= [1 - \frac{200}{1.5 \times 750}] \, e^{-(2.5 \times 20/750)} = 0.822 \times 0.936$$

$$= 0.769$$

$$\bar{M}_t = 1 + (K_t s \Phi_e)$$

$$= 1 + (1.6 \times 0.769 \times 0.10) = 1 + 0.123$$

$$= 1.123$$

$\sigma_v/\bar{V}_z = \sigma_v/\bar{V}_{20} = 0.215$ Table 3.1.5.4

$$M_t = 1 + \frac{K_t s \Phi_e}{[1 + 3.7\sigma_v/\bar{V}_z]} = 1 + \frac{0.123}{(1 + 3.7 \times 0.215)} = 1 + 0.069$$

$$= 1.069$$

3.1.8 Design wind speed with direction of wind. Where sufficient meteorological information is available the gust wind speed at a site may be adjusted for specific wind directions. For some of the major population centres this information has been obtained and is given in Table 3.1.8.